With the support of the
Erasmus+ Programme
of the European Union

University of Évora

ARCHMAT
(ERASMUS MUNDUS MASTER IN ARCHaeological MATerials Science)

Determining safe laser conditions for the cleaning of historic stained-glasses by laser ablation.

Valérie Treil (44428)

Professor Doctor Nicola Schiavon
University of Évora
Co-supervisor

Professor Doctor Maria Pilar Alonso Abad
University of Burgos
Co-supervisor

Professor Doctor Luis Alberto Angurel Lámban
Institute of Nanoscience and Materials of Aragón
Co-supervisor

Professor Doctor Xermán de la Fuente
Institute of Nanoscience and Materials of Aragón
Co-supervisor

Évora, Portugal, July 2022

MEMBERS OF THE JURY

Pr. Luis Alberto ANGUREL LAMBÁN

Pr. Cristina BARROCAS DIAS

Pr. Rémy CHAPOULIE

Pr. Donatella MAGRI

Pr. Nicola SCHIAVON

Pr. Panagiotis SPATHIS

AKNOWLEDGEMENTS

I am grateful to Pr. Nicola Schiavon for enabling me to investigate this research topic.

I would then like to thank Pr. Maria Pilar Alonso Abad for teaching me the history and styles of historic glass windows as well as showing me around the city of Burgos cases studies of every time period. Thank you also for supervising the historic part of my report.

I would like also to vividly thank Pr. Luis Alberto Angurel Lambán and Pr. Xermán de la Fuente for teaching me the concepts, trusting me, and their support throughout my stay with them.

Thank you as well to the whole team of the Institute of Nanoscience and Materials of Aragón (INMA, CSIC-University of Zaragoza) laboratory for their help and friendship, especially to Evan Maina Maingi and Md Ashiqur Rahman.

CONTENTS

LIST OF FIGURES

LIST OF TABLES

Determining safe laser conditions for the cleaning of historic stained-glasses by laser ablation

ABSTRACT

New ultra-short pulsed lasers open new opportunities in the developing of new safe restoration techniques to be applied in stained-glass samples. The pulse duration that are available limit the volume of the sample that it is affected when these lasers are focused on a surface. This allows developing laser cleaning protocols that facilitates the elimination of external layers without deteriorating the layers that are below them, in this case, the glass or the grisaille.

In this work, the use of a 238 fs UV laser has been studied. It has been determined that this laser can induced two types of damage on the glass. A mechanical one associated with the ablation of the sample surface and an optical one, associated with a change in color that modifies the transmittance spectra of the glasses and increases the absorption level in the UV range of the spectra.

The mechanical and optical damage thresholds have been determined on microscope slides and on contemporary stained-glass samples with different colors. In colorless samples, the damage thresholds can be measured using the Lui method that allows to measure the size of the laser beam and the level of energy to damage the sample.

Using these results, it has been possible to define some laser cleaning protocols on stained-glass samples painted with permanent ink. Good results are obtained in a multi-step process in which the initial step is performed with a higher level of energy in order to remove a high percentage of the ink layer and after the cleaning is finished using several steps with energy levels below the optical damage threshold.

KEY WORDS

Stained-glass, damage, laser interaction, energy threshold, conservation.

Determinação de condições seguras de laser para a limpeza de vitrais históricos por ablação a laser

RESUMO

Novos lasers pulsados ultracurtos abrem novas oportunidades no desenvolvimento de novas técnicas seguras de restauração a serem aplicadas em amostras de vitrais. A duração do pulso disponível limita o volume da amostra que é afetado quando esses lasers são focados em uma superfície. Isso permite desenvolver protocolos de limpeza a laser que facilitam a eliminação de camadas externas sem deteriorar as camadas que estão abaixo delas, neste caso, o vidro ou a grisalha.

Neste trabalho, foi estudado o uso de um laser UV de 238 fs. Foi determinado que este laser pode induzir dois tipos de danos no vidro. Uma mecânica associada à ablação da superfície da amostra e uma óptica, associada a uma mudança de cor que modifica os espectros de transmitância dos vidros e aumenta o nível de absorção na faixa UV dos espectros.

Os limites de danos mecânicos e ópticos foram determinados em lâminas de microscópio e em amostras de vitrais contemporâneos com cores diferentes. Em amostras incolores, os limites de dano podem ser medidos usando o método Lui que permite medir o tamanho do feixe de laser e o nível de energia para danificar a amostra.

A partir desses resultados, foi possível definir alguns protocolos de limpeza a laser em amostras de vitrais pintados com tinta permanente. Bons resultados são obtidos em um processo de várias etapas em que a etapa inicial é realizada com um nível de energia maior para remover uma alta porcentagem da camada de tinta e após a limpeza ser finalizada usando várias etapas com níveis de energia abaixo do dano óptico limite.

PALAVRAS CHAVES

Vitrais, danos, interação laser, limiar de energia, conservação.

AIMS AND OBJECTIVES

The main objective of this work is to develop new restoration techniques that can be used to develop new cleaning protocols to be used in the restoration of stained-glass windows. In principle, these new technologies will be based on the use of ultra-short pulsed lasers.

This work has two main objectives. The first one is to review the state of the art of the knowledge of the process of how historic stained-glasses were made depending on the historic period they were fabricated, how they were gathered, the resulting degradation processes and the current restoration techniques.

The second objective is to define the basis of laser cleaning protocols using UV pulsed lasers with a pulse duration of 238 fs. The use of lasers with these characteristics opens new possibilities because it is possible to control the volume of the material that it is affected by the laser. The objective of this work is to increase the knowledge about the possible effects of this type of radiation on glasses (mechanical ablation, optical damage) and determine which are the damage thresholds for each effect. These data will be also used to define a laser cleaning protocol that can be used to develop safe laser restoration protocols to be used in glass conservation. The work has been started in microscope glass slides and after, it has been transferred to contemporary glasses that are used in the restoration of stained-glass windows. From the analysis if these results, new laser cleaning protocols to be used with historical glassed will be defined.

This master thesis has been divided in five chapters. In the first one, a review about the state of the art of the fabrication technologies, pathologies and restoration techniques that have been used in historical stained-glass windows. Chapter 2 describes the samples that have been used in this work, as well as the processing and characterization techniques. The laser used in this work is a pulsed laser with a gaussian energy distribution. This generates some difficulties in the characterization of the laser parameters that define the cleaning protocols. Chapter 3 shows the main parameters that are required to characterize the laser protocol and how to determine them. The analysis of possible defects that laser can induce on a glass surface have been studied on glass microscope slides. The effects of different laser parameters are discussed in chapter 4. Finally, differences on the glass response associated with the different colors of contemporary stained-glass-windows is presented in Chapter 5. Some laser cleaning protocols have been defined in Chapter 6. Main conclusions of the work are presented in Chapter 7.

Chapter 1: History and Restoration of Stained-glass

A) History

A.1.-Chronology

In order to understand the purpose and the origin of the stained-glass windows, it is essential to review the historic context in which they were developed.

We will here give a brief history of stained-glass-windows focusing on medieval Europe, even though stained-glass has been known since antiquity and early traces of stained-glass windows dating from the 7th century can be found in Syria.

From the 12th to the 16th century

The use of stained-glass to make windows in Europe begins in the 10th century, but this use thrived concomitantly to the diffusion of the gothic architectural movement from the 12th century and the erection of cathedrals with wide openings. The geographical origin of stained-glass windows can be found in northern France and Flanders, then expanded to neighboring region such as Germany, England and later Italy and Spain in the following century.

The stained-glass-widows served several functions: architectural, iconographic, and symbolic.

The first purpose of the stained-glass is to fill the architectural void of a window by protecting the indoor space from the weather, the wind while letting the light pass through.

The second function of the stained-glass is to be the support of an image whether it is some repetitive patterns or a figurative representation of objects and characters. The iconography supported by the stained-glass window can have a decorative purpose or represent religious themes taken from the Scriptures, depending on the nature of the building it is part of. Being a luxury art, stained-glasses windows could be found in every building that held power: religious buildings (cathedrals, churches, monasteries…), private buildings (palaces, castles…) or public buildings (town halls, guilds...).

If placed in a religious building, the stained-glass had also a third function: the one of coloring light. This was a symbolic way to materialize the interaction between the divine world, the sky from which the light comes from, and the terrestrial world. By displaying religious themes brought to life by light, the stained-glass windows where the embodiment of the message of the Christian God to the humans. In the medieval context, every element of the churches' architecture was imbued with symbols. The stained-glass windows were in charge of representing the sky and the characters present in it: the colored enlightened themes enhanced the dichotomy with the tangible world of the spectator. In addition, when the stained-glass was to be seen by the masses in a church for example, it also served a pedagogical purpose as majority of the population didn't know how to read. The stained-glass was a way to give access and illustrate the Scriptures.

However, the stained-glass windows, with their vivid colorful characters and the moving color spots they created in the indoor space were criticized notably the Cistercians lead by Saint Bernard of Clairvaux. They were referred to as source of distraction for the people that prevented them from being fully engaged in the worshipping activity. For this reason, the spaces dedicated to religious people (monasteries, the church Choir) more often displayed non-colored white glasses and symbolic patterns as those people were literate and were already familiar with the Scriptures. Whereas the spaces designed to welcome a more important and diverse public displayed colorful, rich and explicit representations of characters and scenes (temples, the nave of the church). This contrast can be

illustrated by the stained-glass of the basilica-cathedral of Saint-Denis [Figure 1.1] and the priory of Saint-Martin-des-Champs [Figure 1.2].

Figure 1.1: *Basilica-cathedral of Saint-Denis, 12th century, Saint-Denis (France), [source: commons.wikimedia.org, author: Vassil]*

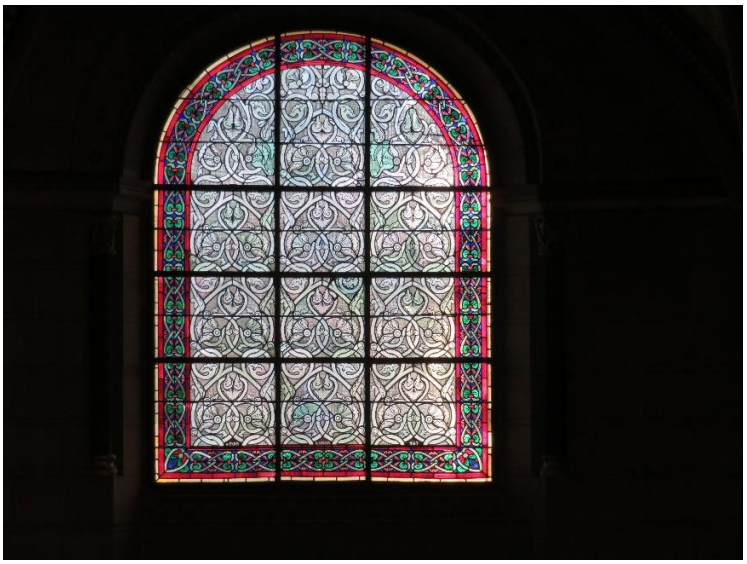

Figure 1.2: *Priory of Saint-Martin-des-Champs, 11th-13th century, Saint-Martin-des-Champs (France), [source: commons.wikimedia.org, author: Sukkoria]*

From the Middle Ages to the Renaissance, a stylistic evolution in the stained-glass window compositions can be noted [Figure 1.3]. Whereas each window was dedicated to once scene and each panel to one character during the Middle Ages, the scenes tend to complexify during the Renaissance. Several lancets and windows can be associated in a single theme to represent complex scenes featuring an abundance of characters and sometimes even perspective in the background decor. It is also from this period that inscription that explicitly indicates the passage of the Bible illustrated could be added at the bottom of the image to help the spectator understand the context of the image.

Figure 1.3: *Cathedral of Segovia (Spain). Gospel nave. 16th century, [source: commons.wikimedia.org, author: GFreihalter]*

From the 16th to the 18th century

The 16th century marks a turning point in the history of stained-glass.

As the Church was the main patrons of the Arts, the Counter-reformation impacted the manufacture of stained-glass windows. The Council of Trent (1545-1563), in the context of the Counter-Reform, stated a tendency for more soberness. In worshipping buildings, small openings, placed in height and displaying few and discreet colors were preferred. Little by little the stained windows were replaced for to more sober colors and symbolic patterns [Figure 1.4]. This change in taste was implemented from the 16th century and diffused though Europe, although the appreciation for the gothic style perdured longer in Spain. This was the beginning of a period of nearly three centuries during which the profession of glaziers disappeared as well as the practical knowledge that they carried. If the case were the former stained-glasses panels were conservated after removal, they were stored and used as a source of replacement pieces in case the new ones got to be damaged. It is not uncommon that a stained-glass panel included pieces from a variety of periods, sometime leading to an heterogenous mix when the colors or patterns the pieces don't always match. When a piece of glass broke and, the hole could also be filled with cement.

Figure 1.4**:** *Emblematic window, Renaissance (c.1550), Musée National de la Renaissance (Écouen), [source: commons.wikimedia.org, author: GFreihalter]*

During this unfortunate period of roughly three hundred years old, not only fabrication knowledge was lost but also practical knowledge about how to monitor, care and repair the stained-glass windows. The only treaties and manuscripts that consigned the recipes and technical indication for the Middle Ages were kept in the archives or religious libraries of the monasteries. This did not facilitate the access to the knowledge to the persons in charge of the daily care of the stained-glass windows as they may not know how to read or they didn't even know were to look for information.

From the 19th to the present day

It is not until the second half of the 19th century that the interest for stained-glass was reborn along with the apparition of the artistic movement of Art Nouveau.

In place of the medieval workshops, International Houses devoted themselves to the restoration of the historic stained-glass windows that had been neglected, but also to the fabrication of innovative creations. The old recipes had to be recovered thanks to the recollection of archives, then were tested to reinvent the crafting expertise. Some artists and craftsmen paid tribute to the medieval and Renaissance works of art by imitating the choice of colors, the shapes of the glass pieces and the iconographic composition; but there was also great innovation in the range of glass textures and color palettes with the use of new oxide mixes. The Mauméjean family (France), Franz Xaver Zettler and Joseph Mayer (Munich), Jean-Baptiste Capronnier – Capronnier Studio (Brussels), and Louis Comfort Tiffany – Tiffany Studios (New York) can be mentioned as some of the main international studios and glaziers.

The Art Nouveau enable a renewal of the patterns but also of the variety of use of the stained-glass. Stained-glass is not only constrained to windows, but appears in staircases, roofs, and facades, and doors. Stained-glass can also be used without architectural function, but as a pure element of decoration in lamps or decorative panels on the walls or ceilings. When used indoors, stained-glass is easy to maintain, to install and to transport (some panels are installed in independent frames easily

movable), and less likely to be degraded. However, it has to be mentioned that decorative indoors panels have to be enlightened on purpose, which can lead to thermal degradation.

The 19th and 20th centuries also witness a diversification of the type of buildings in which stained-glass-windows are displayed: not only religious buildings and private houses, but also theaters, operas, casinos and art centers, trains stations, banks, concert halls, metropolitans' entrances, etc. The possession of stained-glass works of art is still associated with prestige [Figures 1.5 and 1.6].

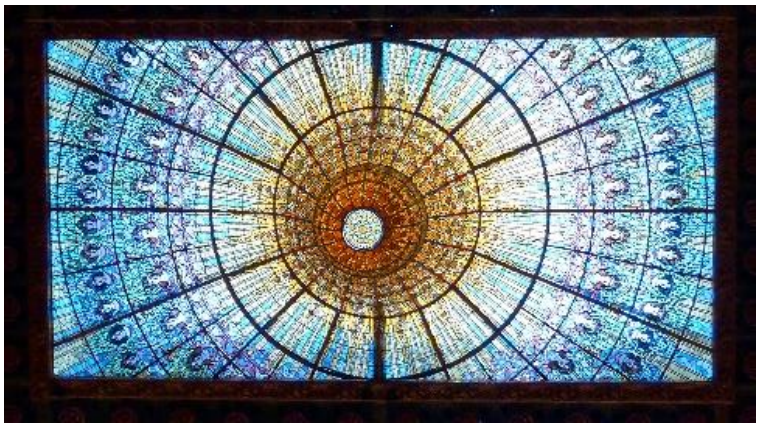

Figure 1.5**:** *Music Palace, 1908, Barcelona (Spain), [source: commons.wikimedia.org, author: Tony Hisgett]*

Figure 1.6: *Colon Theater, 1908. Buenos Aires (Argentina), 1908, [source: commons.wikimedia.org, author: Sergio Moises Panei Pitrau]*

It is also from this period that the craft of stained-glass began to reach other continents than Europe, and in particular North and South America.

In the Middle East, new buildings such as the Nasir al-Mulk Mosque (1876-1888) in Iran, featured traditional Orossi (or Orsi) stained-glass windows [Figure 1.7].

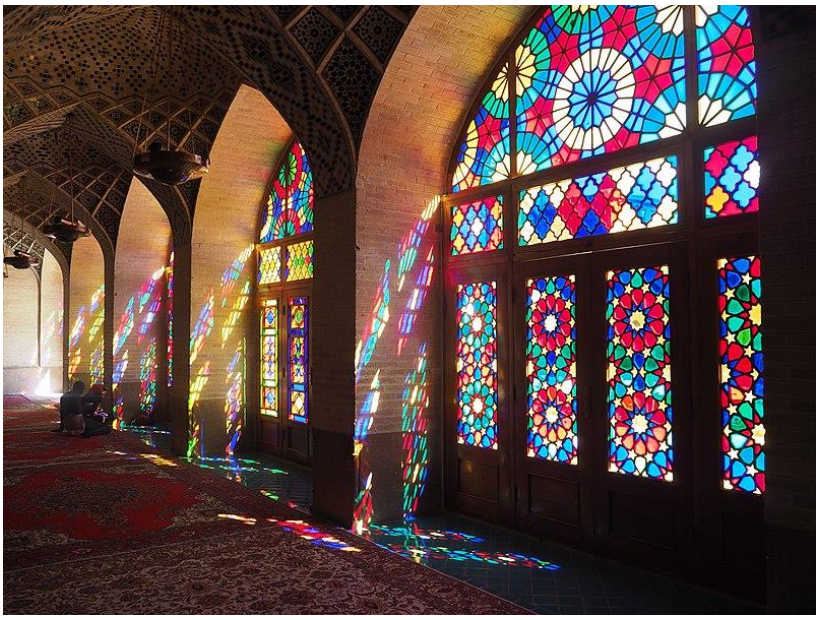

Figure 1.7: *Nasir al-Mulk Mosque (Iran), [source: commons.wikimedia.org, author: Scott Edmunds]*

Along with the experiments in texture and colors, new techniques and types of glasses were also developed from the end of the 19th century and all throughout the 20th century. During the 1870's, John Lafarge introduced opalescent stained-glass windows, by transferring the technique already used for tableware to flat sheets [Figure 1.8].

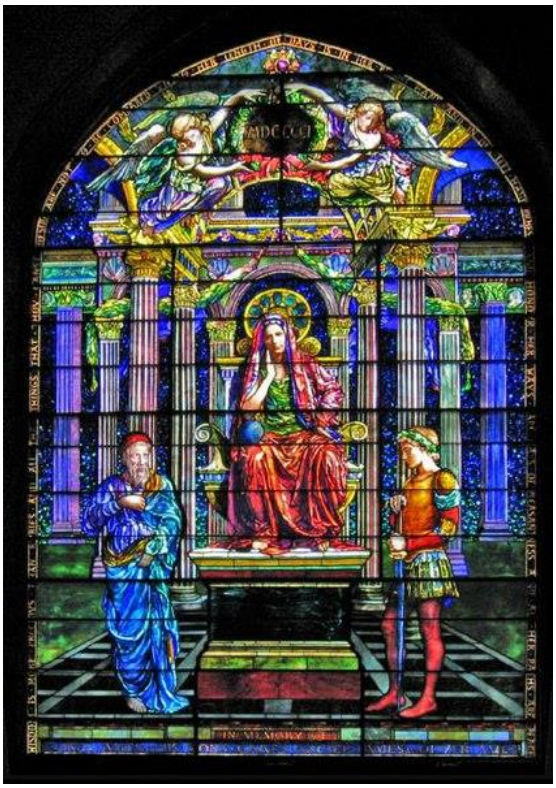

Figure 1.8: *"Figure of Wisdom" stained-glass window in Unity Church, North Easton, by John Lafarge, 1901, [source: commons.wikimedia.org, author: Daniel P.B. Smith]*

During the 1930's, Jean Gaudin invented the "Dalle de Verre" technique, where the pieces of stained-glass are not inserted in lead armatures, but imprisoned in a matrix of cement (or later in epoxy resin), and was soon imitated by others. [Figure 1.9] This technique allows to create what was referred to as "mosaic windows".

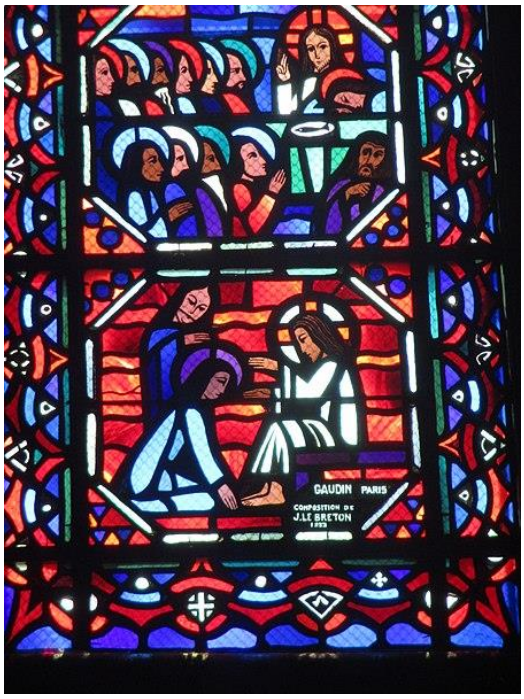

Figure 1.9: *Art Deco Stained-glass window by Lebreton, 1933. Sacré-Coeur (Cathedral of Amiens), [source: commons.wikimedia.org, author: Thomon]*

Among the new types of glasses developed during this period, lava glasses (imitating an incandescent effect), the enamel glasses (decorated with vitreous paint), bubbled glasses, and combined glasses can be quoted.

After the two World Wars, the interest for new stained-glass work diminished and the majority of the production demand now mainly concerns the restoration of historical stained-glass windows.
Nowadays, experiments are still conducted to better the quality of the glasses and the paint in resistance, durability and closeness to the original medieval techniques or developing innovative properties for the glass such as resistance to high temperature (fire). Research is also focusing of the study of stained-glass deterioration and the development of new restoration techniques.

A.2 Fabrication

Since the 12th century, the fabrication steps of stained-glass windows remained the same. Apart from stylistic changes, the only technical changes come from the composition of the glass and the paint.

Stained-glass window creation steps

The main steps to make a stained-glass window are the followings: the design of the cartoon, the cutting of the glass, the painting, the firing, the insertion of the pieces into the lead structure, the setting of the panels in the architectural opening.

It should also be noted that the glassmakers were itinerant, but the workshops were stable and were normally based in a main population nucleus -usually cities-.

In the medieval glaziers' workshops, each person was responsible and dedicated to one of the fabrication steps. The master is often the one to design the patterns on the cartoon, in charge of presenting the preliminary drawings to the sponsor and concluding the contract, but also of applying the paint and monitoring the oven temperature, the cutter, the leader, and the settler or mason.

The first step is to drawn the image that will be represented on the stained-glass window at the smaller scale and decide the types of colors and their location according to the specifications of the sponsor. The sponsor that is paying the work chooses the artist, the scenes and the characters to be represent the type of pigments and the quality of the glass purchased. Once the design has been accepted, the design can be reproduced on paper at real scale.

The leader plans the division of the drawing into panels and pieces taking into account the aesthetic as well as mechanic considerations. The cutting should underline the main elements of the composition without hindering its lecture while providing for a structure that will resist to the weight of the total window and the assault of the wind.

The cutting map is then used to cut the pieces of glass by transparency according to the tracing. To cut the glass, a ray is formed thanks a hot iron tip [Figure 1.10], a diamond tip, or glass scissors used when the glass sheet is still hot. The pieces are separated using tweezers, then can be decorated with vitreous paint. Because the paint contains silica, it will adhere to the glass by fusion during a firing step after paining. The paint can be added to by layers with paint brushes, or part or the paint can be removed thanks to a wooden point. The final colors of the paint are revealed after the firing as the metallic pigments are oxidized. The temperature of the oven should be controlled and remain constant for the piece to ensure homogenous color plain swaths and prevent the apparition of stains or degraded zones.

Figure 1.10: *A heated dividing iron causing a crack to form on a glass sheet. (Image from [Carson Pastan2019])*

The pieces are joined by insertion in H-shaped lead bars with addition of putty. Once the different panels of stained-glass that compose the window are finished, they are settled into the wall opening, and fixed with cement. The different panels are linked by iron structural bars. Additional horizontal iron supportive bars are placed in front of the panels next to the glass. They serve as a mechanic support that prevent the panels when they bend because of the wind force or the gravity.
Protective iron grids can be installed on the exterior side to protect the stained-glass window from projectiles (hail stones, branches) and birds, mainly.

Glass making

Glaziers are not in charge of making the glass they used and are provided with glass sheets by glass makers. Understanding how the glass is made allow us to explain the differences in resistance, durability and degradation.

Glass is a mix of silica (coming from sand), fluxing and stabilizing agents (from salts and wood ashes), and eventually coloring agents (metallic oxides from ores). This mix is heated inside a ceramic crucible into an oven at high temperature for the components to melt. While malleable, the glass maker blows air in the middle of the paste thanks to an elongated blowing pipe. This creates a sphere than can be elongated into a cylinder by swinging. The edges are cut and the cylinder is opened in its length then flattened to obtained a glass sheet. The glass is then cooled rapidly enough for the matter to stay amorphous.

During the blowing step, bubbles of air are introduced into the glass bulk. During the Middle Age this characteristic of the glass was appreciated for the bubbles induced bright rays of light that crossed the colored piece and brought life to the pattern represented. However, the more the bubbles the more fragile the glass. From the 16th century, sponsors started to demand high quality glass with fewer bubbles. The sponsors checked the quality of the purchased glass then checked the final stained-glass windows.

During this period, glass factories produced this material using different types of techniques. The most common were “hand-blown cylinder and crown glass.

Types of coloring

There are two ways to color the glass: it can be colored in the mass during its fabrication, or it can be painted afterwards.

At first from the 12th century glass was made in five different colors: red, blue, green, yellow and “white” or to say colorless. Then the glass pieces could be painted with a dark paint called grisaille. Grisailles can be found in different tones: gray, brown, dark green, dark red. The number of layers of grisaille applied and the concentration of the paint permit to obtain different shades of the same color. In the late 13th century appeared the use of silver stain (a mix of silver compounds complaining notably silver nitrate) that offered a way to make yellow or green swaths if used over white or blue glass respectively [Figure 1.11].

Figure 1.11: *Saint Peter, National Museum of Middle Ages of Paris, 1500-1510, [source: commons.wikimedia.org, author: Jastrow]*

Other ways to create a color pattern on the same piece of glass are the scrapping of ruby red, and the "jeweled" inserts. Because the copper oxide used for red is very intense and resulted too dark if inserted in the bulk of the glass, the way to make red wad to simply coat one side of a white glass and then fire it. If this layer is scrapped in certain areas, white or yellow patterns (if yellow silver stain is then applied) inside the red piece can be obtained. On the other hand, the "jeweled" insert technique consists in carefully drilling a hole into the piece of glass, then insert a piece of another color inside and seal it with a lead joint.

The 16th century showed the apparition of what can be referred as "pictorial windows". Indeed, a variety of vitreous paints was developed. The combination of several metal oxides gave offered new shades of colors to be painted: pastel color, purples and pinks. [Figure 1.12]. These technical advances allowed for larger pieces of painted glass and less lead need for the structure. As the glass is more resistant in time than lead that bends, the result stained-glass in thus more durable. However, it has to be noted that in case or high temperatures, such as in accidental fires, the complex paints containing several oxides are less resistant than the simpler medieval ones.

Figure 1.12: *Stained-glass window from Saint-Martin Catholic parish church in Herblay, 16th century, (France), [source: commons.wikimedia.org, author: GFreihalter]*

Design parameters and conception

When the glaziers design a stained-glass window, there are a number of parameters that have to be considered for their creation to fill in the requirements of the previously mentioned functions: closure of a wall opening, transformation of the penetrating light, and representation a theme.

To address the first architectural and practical function, the height of the window has to be considered. The higher the windows, the stronger the wind. The direction of severe weather has to be studied: depending on the direction from which the wind and the rain are coming, some of the stained-glass windows will be reinforced with supportive bars and lead network. The natural tendency of the stained-glass structure to bend with time has to be minimized to prevent the glass-pieces from falling. Moreover, the type of the aperture has to be taken into account to design the cut of the pieces and the structural bars: the physical forces differ if the opening is a thin and elongated window or a rose window with stones compartments, the latter being more resistant.

The aesthetic and symbolic function of transforming the light has to be designed taking the orientation of geographical orientation of the window.
INTENSITY. The light will be softer if facing the North and brighter is facing the South. Thus, pale and color should be employed in Northern window. Pastels and yellow with let this soft light come enter without any disturbing burst of light. On the contrary, dark and saturated colors (bold red and blues) should be placed in southern windows so they can be invigorated by the bright light.

SOURCE COLOR. The stained-glass windows can also benefit from how the daylight changes in color during the day, from yellow at down, to white au zenith, to orange and red at dusk. In such a way, a stained-glass window featuring a scene with blood positioned toward west will give an eve mire vivid impression.

ASSOCIATION. The choice of adjoining colors is deliberate: once the light has passed through eh stained-glass the rays fall on the ground or walls into blurry stains of colors. To ensure a high contrast even then, and prevent the mixing of hues, opposite colors must be associated: red with green, blue with orange, yellow with purple. A warm color in association with a cool color.

TEXTURE. The irregularities of the glass can be taken advantage of: the texture of the glass surface to give sparkling to the pattern, and the changing thickness of the glass to give a watery effect.

In order to provide their function of representation, the distance at which the panel will be observed should be taken into account. The more complex and detailed scenes should be features at the bottom of the window whereas the higher par should be reserved more simpler and more symbolic patterns. Moreover, the scale of the objects and the proportions of the characters should be adapted to the distance at which they can be observed and correct the deformation due to the distance.

Finally, the more important details can be underlined by being reproduced with grisaille on the exterior part of the glass. This can also be used to give a three-dimensional effect to the composition.

B) Types of glasses

According to Agua *et al.* (Agua *et al.*, 2022) the main glass groups are soda lime silicate (Na_2O-CaO-SiO_2), potash lime silicate (K_2O-CaO-SiO_2) and potash lead silicate (K_2O-PbO-SiO_2) glasses. The most frequent in stained-glass windows are soda lime (usual in Renaissance) and potash lime silicate (normally in medieval times) glasses. In transitional chronological periods, glasses have an intermediate chemical composition between both.

In glasses from stained-windows the main forming component of the glass network is silicon oxide (SiO_2). Sodium and potassium oxides (Na_2O y K_2O) play the role of glass network-modifiers since they low the melting temperature and hence they facilitate the glass making. Calcium oxide (CaO) behaves as a glass network-stabilizer. Other components are also identified in glasses from stained windows. They are minor components such as colorants (chromophores) (Agua *et al.*, 2022), bleaches, fining agents and opacifiers. The most frequent are colorants which are usually transition metals. Regular raw materials used to melt traditional glasses were: quartz sand (SiO_2), natural natron (Na_2CO_3 $10H_2O$), halophytic plant ashes (Na_2CO_3), forest plant and trees' ashes (K_2CO_3) and natural limestone ($CaCO_3$).

The typical chemical composition (expressed as oxides) of a glass from a medieval stained-glass window (11^{th}-15^{th} centuries) is shown in Table 1.1. Müller et al. (1994) classified chemical composition of Medieval and Renaissance glasses into five groups (Table 1.2).

Oxide	SiO_2	Al_2O_3	MgO	CaO	Na_2O	K_2O	P_2O_5
wt.%	45-55	0-1	0-1	15-35	0-2	15-25	0-4

Table 1.1: Average chemical composition of glasses from medieval stained-glass windows (11^{th}-15^{th} centuries).

Oxide	$CaO/K_2O<2$	$CaO/K_2O>2$	12^{th} century	Medieval Ages	Renaissance
SiO_2	45-55	45-55	60-75	30-40	55-70
CaO	15-25	25-35	1-6	5-20	10-20
K_2O	15-25	10-15	5-8	5-20	2-8
Na_2O	0-2	0-2	10-18	0-1	2-8
PbO	0-1	0-1	0-1	10-50	0-1
P_2O_5	0-4	0-4	0-4	0-10	

Table 1.2: CaO/K_2O ratio and average chemical composition of glasses from stained-glass windows of different chronologies (after Müller et al., 1994).

C) Glass deterioration

Intense alteration of glasses results in their deterioration, due to long periods of time enhances a chemical corrosion which, weakens mechanical integrity of glasses, other materials of the stained window, mainly.

Glass corrosion is also connected with alteration of its original colors and diminishing of its transparency, which enhances the formation of iridescent layers and/or detachments (García-Heras et al., 2003a, 2003b; Villegas *et al.*, 2008; Carmona *et al.*, 2001, 2009).

Causes for glass deterioration can be classified in intrinsic (due to the glass nature itself) and extrinsic (due to the glass environment).

C.1 Intrinsic causes of deterioration

The main one is its chemical composition. Other intrinsic causes are homogeneity defects, mechanical stresses both in bulk glass and in its surface, hurts and microcracks, etc. as well as problems derived from former interventions made by non-specialists.

C.2 Extrinsic causes of deterioration

The extrinsic causes have chemical, physical and biological origin.

CHEMICAL ORIGIN: The main ones are humidity or water condensation, rain, frost, etc. Environmental pollutants coming from both outdoor (CO_2, SO_x, NO_x) from road traffic, engines, combustion, factories, thermal power plants, etc., and indoor environment (formic and acetic acids, formaldehyde, candles smoke, heating systems, cocking foods, etc.) are also causes for glass chemical deterioration. Also, the longer the stay of a glass under an aggressive environment, the higher will be its deterioration, and even the same about temperature.

PHYSICAL ORIGIN: They are related with mechanical problems in glass due to its brittleness against external stresses (mainly bending stresses), vibrations or wind pressure. Others can be the thermal conditions (such us extreme environmental temperature, seasonal thermal cycles and daily thermal changes), or artificial lighting sources, solar radiation intensity and some other optical factors.

BIOLOGICAL ORIGIN: They are mainly connected to the presence of microorganisms, fungi, bacteria, etc. When glasses are previously altered or degraded by chemical agents (humidity, pollutants) they become very sensitive against colonization by microorganisms, lichens and other biological agents who are able to survive on the glass surface. In several cases, they deposit upon the glass surface the products of their metabolism. Consequently, microorganisms penetrate progressively into bulk glass even up to a depth of several millimeters. Cleaning and restoration of glasses degraded by biological colonization are limited and these pathologies are considered irreversible (Carmona et al., 2005a, 2006a).

C.3 Pathologies of stained-glass windows

The most common alterations are due to vandalism actions, deposits of dirty and soot, detachment of masonry and lead frames, loss of transparency and masking of original colors are very frequent. These problems cause artistic devaluation and difficulties for its iconographic understanding.

Other alterations are atmospheric pollution gives rise in grisailles and pictorial layers on glasses; bird droppings with deposits upon the outdoor side of stained-glass windows because of its very basic pH; corrosion on the substrate. All of them make cleaning operations could be a serious risk for grisailles and surface colorings.

Gypsum remains, mortar and other construction materials used for stained-glass windows installation or from the adjacent walls can provide conservation problems. The glass surface can be altered due to the basic nature of such materials.

D) Cleaning, restoration and preventive conservation

The procedure for cleaning and restoring stained-glass windows has different phases:

Cleaning: Mechanical releasing of dirty deposits using soft brushes and paintbrushes made of natural hair.

Sealing of cracks and edges, union of broken fragments: Using adhesives and cementitious materials especially designed for glass (cellulosic compounds, epoxy, vinyl, acrylic, polyester, polyurethane, cyanoacrylate resins, etc.). This solution is reversible.

Fixation and consolidation of grisailles, polychromes and other pictorial layers: Specific adhesives and substances for these pictorial layers should only be applied if they are reversible (Carmona et al., 2006e).

Re-composition of iconographic elements: Only possible when corresponding historic and artistic documentation is available.

Repairing and/or renewing of lead cames and other metallic elements: To preserve original metallic elements of the stained-glass window as much as possible. If it's necessary substitution by modern elements, they should be adapted to the whole aesthetics of the stained-glass window and the building, and properly protected with primes and anticorrosive paints (García-Heras et al., 2003b, 2004, 2006b, 2009; Peña-Poza et al., 2013).

Protective coatings: Traditional preservation was focus on protective coatings strategy based on acrylic resins, silicones, alkoxysilanes, etc., but nowadays it is not recommendable, because any coating does directly affect the original glass surface, and could cause an alteration of natural weathering conditions of glasses with negative consequences. The conservative criterion is to avoid any kind of coating to be directly applied on the glass surface (Carmona et al., 2003, 2004, 2006f).

Protective glazing: currently the most accepted strategy is installation of exterior protective glazing. The stained-glass window is set back at about 15-20 cm towards the building inside and in the free place an isothermal glazing is installed. This creates a natural ventilation chamber and avoid any risk of condensation upon the stained-glass window, even atmospheric agents, vandalism, pollution, etc.

Preventive conservation: cleaning and restoration tasks would only have a temporal validity if a preventive conservation plan is not stated and carried out. The plan must consider frequent revisions of all the stained-glass window elements of both sides and the environmental characteristics.

Chapter 2: Experimental

A) Sample materials

Six contemporary stained-glass samples of different colours (blue, yellow, purple, green, red, and colourless) were selected (Figure 2.1). These samples were supplied by the glass factory of Verrerie de Saint-Just, located in Saint-Just-Saint-Rambert, in Loire (France). This factory was founded about 189 years ago. Currently, Verrerie de Saint-Just glass maker is a reference supplier of glass and stained-glass in Europe. The samples have a thickness of 3 mm and a rectangular shape with the dimensions indicated in Table 2.1. It must be noted that the glasses are not perfect: they contain bubbles of heterogenous dimensions. The range of bubbles dimensions is also included in Table 2.1.

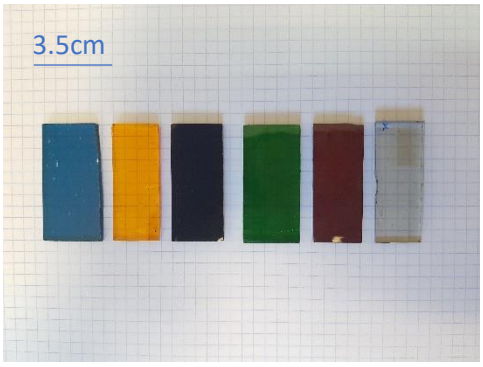

Figure 2.1: *Samples of six modern colored stained-glasses. From left to right: blue, yellow, purple, green, red, and colorless slides.*

Sample color	**blue**	**yellow**	**purple**	**green**	**Red**	**colorless**
Dimensions (cm)	4x2-1.8	4x1.55	4x1.8	4x1.9	4x1.6-1.55	4x1.5-1.6
Smaller Bubbles (mm)	1x0.3	1x0.3	1-3x1	1x0.5	1x0.3	1x0.3
Bigger bubbles (mm)	3x0.5	8x2	1-3x1	3x2 Only one	9x2	3x1

Table 2.1: *Samples of six modern colored stained-glasses. From left to right: blue, yellow, purple, green, red, and colorless slides.*

In order to characterize the effects of laser radiation with glass, additional experiments have been performed in microscope glass slides (Thermo Scientific) with dimensions 1 x 25 x 75 mm^3.

B) Laser instruments

Two different laser systems have been used in this work (Table 2.2). A picosecond (ps) near-infrared laser (PowerLine Pico 10-1064, Rofin-Sinar, Germany) with a wavelength of 1064 nm, a pulse duration of 800 ps and a maximum output power of 8W, coupled with a galvanometer mirror system. The pulse repetition rate can be modified between 250 and 800 kHz and the waist diameter of the laser beam ($1/e^2$ criterium) is approximately 80 µm, as deduced following the D^2-method proposed by Liu [Liu1982]. The second one is a femtosecond (fs) laser (Carbide model, Light Conversion, Lithuania), also coupled to a galvanometer mirror system (Direct Machining Control, UAB, Vilnius, Lithuania) (Figure

2.2). Treatments were performed in this case at 343 nm, with a pulse duration of 238 fs, a maximum output power of 11.1 W and a beam diameter of approximately 30 µm. The output power of the laser can be controlled by the attenuation percentage. Figure 2.3 shows the calibration curve of the laser when a resonator frequency of 200 kHz is used. Pulse frequency can be modified between 1 kHz and 1 MHz and the system offers the possibility of selecting the final frequency using the pulse peak divider option.

Laser model	Carbide model, Light Conversion, Lithuania	PowerLine Pico 10-1064, Rofin-Sinar, Germany
Wavelength	343nm	1064nm (IR)
Nominal power	11.1W	8W
Pulses' width	238fs to 10ps	800ps
Frecuency range	1 kHz to 1 MHz	250 kHz to 800 kHz
Beam diameter	30µm	80µm

Table 2.2: *Specifications of the laser systems used in this work*

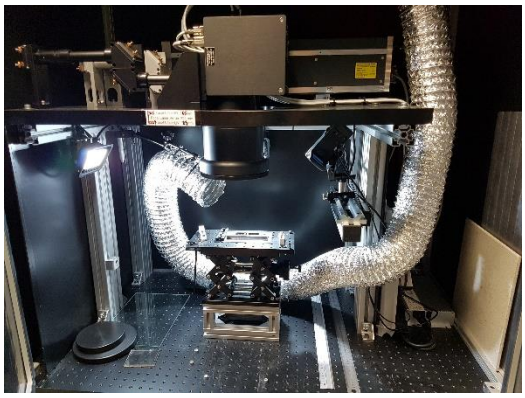

Figure 2.2: *Image of the fs laser and galvanometric mirror system used in this work.*

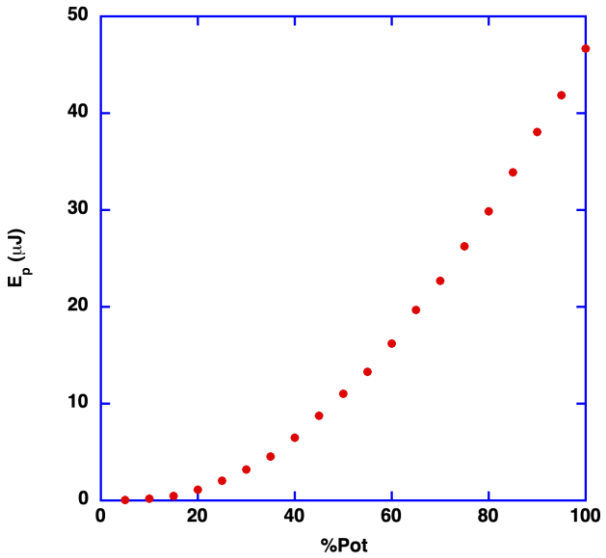

Figure 2.3: *Calibration curve of the fs UV laser for a resonator frequency of 200 kHz.*

The fs laser offers the possibility of using the pulse peak divider (PPD) option. As it is shown in Figure 2.4, it works as a shuttle that allows to select a single laser pulse in a given sequence. For instance, if PPD=20, it means that we are going to use one pulse every 20. If the laser resonator works at 200 kHz,

this means that the effective frequency for the laser treatment is 10 kHz. With this option, it is easier to modify the frequency of the laser treatments without modifying the pulse energy.

Laser scanning was performed in two different modes: beam scan and burst. In the beam scan mode, the laser scans the surface at a given speed, controlling also the distance between two consecutive scan lines with the galvanometric mirror system. The burst mode consists on a spot-by-spot scanning process with adjustable laser parameters. The laser system produces a sequence of a defined number of pulses (a burst) controlling the repetition rate. A single burst is incident at a given position and the distance between the positions, the energy of each individual pulse and the number of pulses in a burst can all be set by software.

Figure 2.5 shows the experimental arrangement used to perform the laser treatments on glass. It is important to have in mind that in many cases glass is near transparent to laser radiation. In this case, the laser can reach the material where the glass has been placed, producing ablation on it. Nanoparticles that are generated during the ablation process can be placed on the back side of the glass [Molina2021]. For this reason, glass has been placed on a support that assures a gap of several millimeters between the glass and the material behind it.

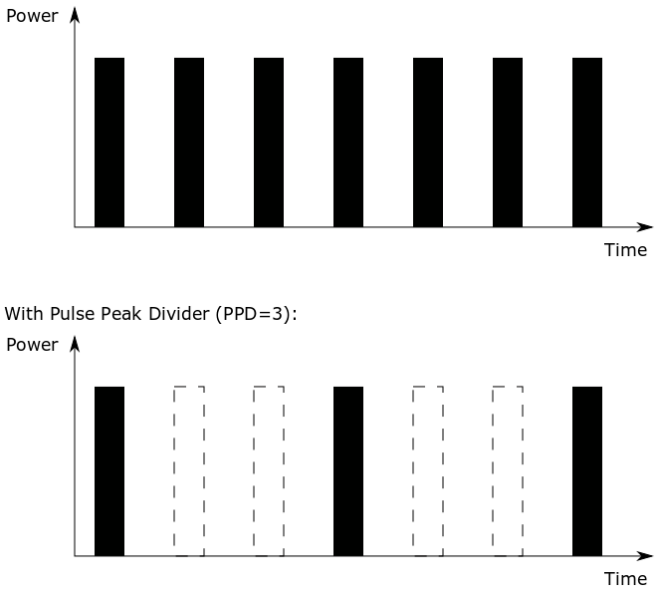

Figure 2.4: *Scheme illustrating the principle of the pulse peak divider (PPD)*

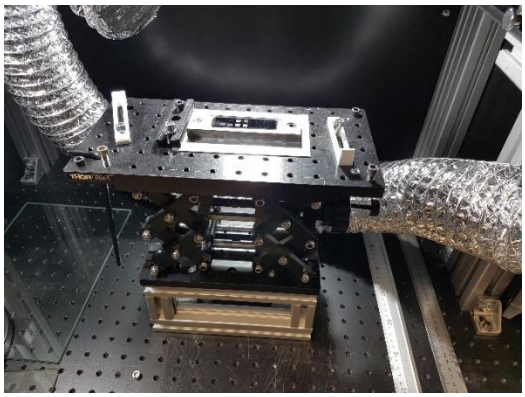

Figure 2.5: *Image of the arrangement used to place the glass for the laser treatment.*

C) Characterization techniques

Spectrometer

The transmittance and absorption values in the UV-Vis-nIR range, in particular, between 300 and 1100 nm, were characterized using a StellarNET Miniature Spectrometer (Figure 2.6). A SL1-CAL light source, 0.6 mm in diameter and a cone angle of 25.4º at the output of the optical fiber and specifically configured for irradiance calibrations in the 300-1100 nm range, was used. Transmittance tests were carried out with an integration time of 5 ms, averaging 100 scans.

A special sample holder has been designed in order to fix the glass samples during the experiments (Figure 2.6.c). This holder maintains the glass surface perpendicular to the illumination direction. This improves the reproducibility of the measurements.

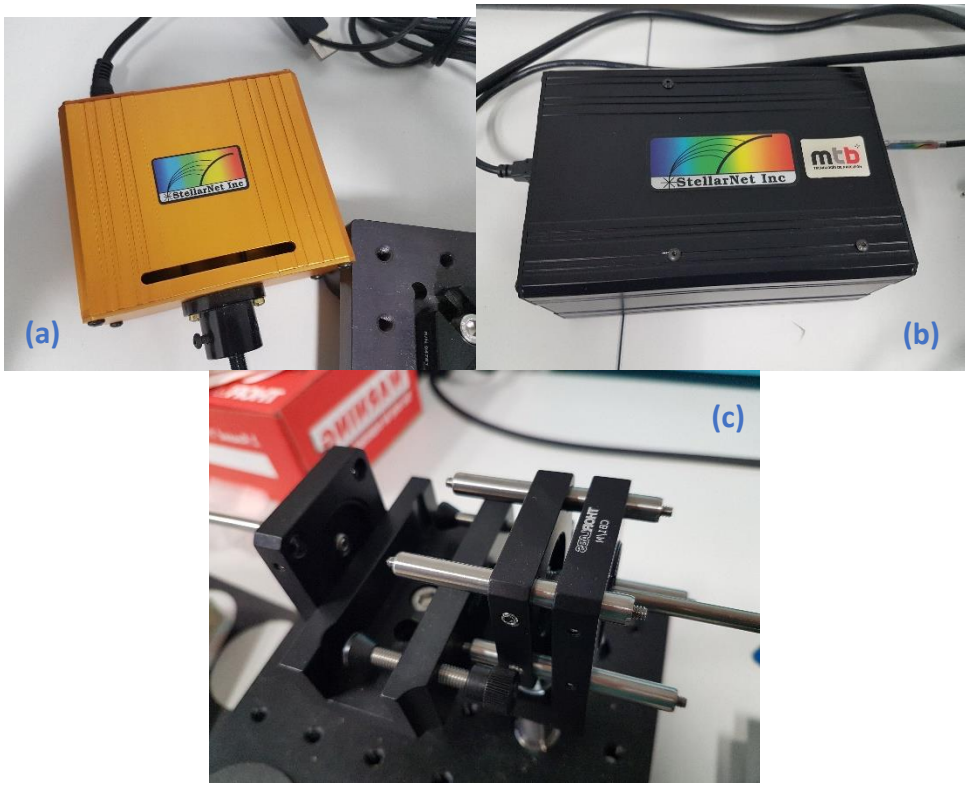

Figure 2.6: *Images of the different components of the spectrometer: (a)SL1-CAL light source, (b) StellarNet unit and (c) sample holder*

Confocal microscopy, and optical microscopy

An initial characterization of the surface after laser treatments has been performed using optical microscopy. A digital USB microscope and a ZEISS SteREO Discovery.V8 (8:1 manual zoom range) microscope (Figure 2.7) were used.

Figure 2.7: *Photograph of the ZEISS SteREO Discovery.V8 optical microscope used in the surface morphological observation of the glasses.*

Topography of the surface before and after laser cleaning was measured using a confocal microscope (Sensofar PLμ2300) (Figure 2.8). A confocal microscope provides sharp images of surface analysis that would otherwise appear blurred when viewed with a conventional microscope. This is achieved by excluding most of the light from the specimen that is not from the microscope's focal plane. A confocal microscope allows to build three-dimensional (3D) reconstructions of a volume of the specimen by assembling a series of thin slices taken along the vertical axis.

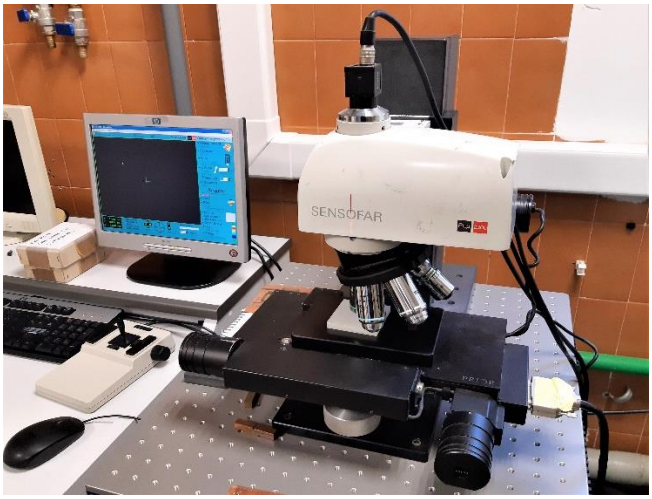

Figure 2.8: *Image of the confocal microscope used in this work*

Chapter 3: Determination of beam size and laser damage energy threshold

A) Characterization of gaussian laser beams

Most of the laser beams have a gaussian energy distribution. In the case of a pulsed laser, laser emission is performed at a given average power, P, with pulses at a given repetition frequency, f_{rep}, and a given pulse duration, τ_p. The main parameters that are used to characterize the pulse are:

The **Pulse Energy** (E_p) can be calculated as the energy emitted by the laser in one second (P) divided by the number of pulses this period of time, given by f_{rep}:

$$E_p = \frac{P}{f_{rep}}$$

Average Fluence (F_p) corresponds to the pulse energy per unit area:

$$F_p = \frac{E_p}{A}$$

where A is the area of the laser beam.

Irradiance (I) is defined as the power per unit area of one pulse with a pulse duration, τ_p:

$$I = \frac{E_p}{\tau_p\, A} = \frac{F_p}{\tau_p}$$

In order to determine all these magnitudes, we need to define the area of the laser beam. Figure 3.1 shows the spatial distribution of the fluence assuming a circular gaussian profile given by

$$F(r) = F_{max} \exp\left[-2\left(\frac{r}{r_0}\right)^2\right]$$

With this definition, the beam size is associated with r_0, point where the energy is F_{max}/e^2. This is known as the $1/e^2$ criterium for gaussian profiles size definition [Liu1982].

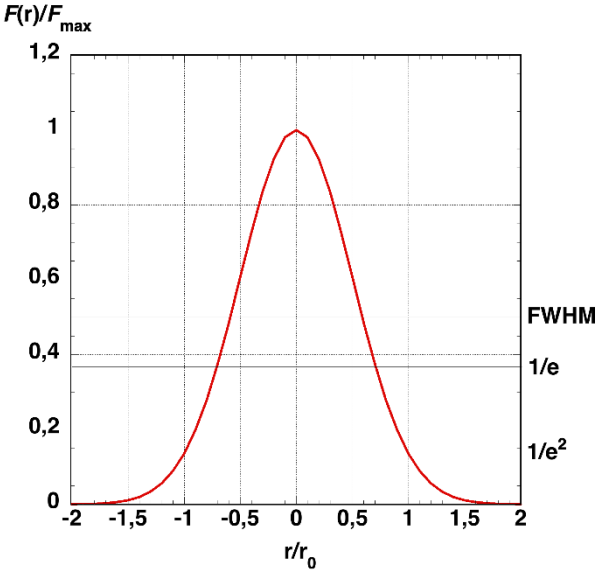

Figure 3.1: *Spatial fluence distribution in a circular gaussian laser beam*

If we integrate the gaussian distribution, we can derive that the maximum fluence value at the center of the beam, F_{max}, is two times the average fluence, F_p.

Sometimes, the beam profile is not circular and has an elliptical shape. In this case, the above equation can be transformed in:

$$F(x,y) = 2\,F_p \exp\left[-2\left(\frac{x}{a}\right)^2\right] \exp\left[-2\left(\frac{y}{b}\right)^2\right]$$

where *a* and *b* are the semiaxis of the ellipse.

B) *Liu method*

Using the gaussian energy distribution, Liu proposed a method to experimentally determine the size of the laser beam. This method also provides information related with the damage threshold on the material because it assumes that the footprint generated by the laser on the material is associated with the part of the beam where the fluence is higher than the damage threshold, F_{th}, as it is represented in Figure 3.2 for three levels of fluence.

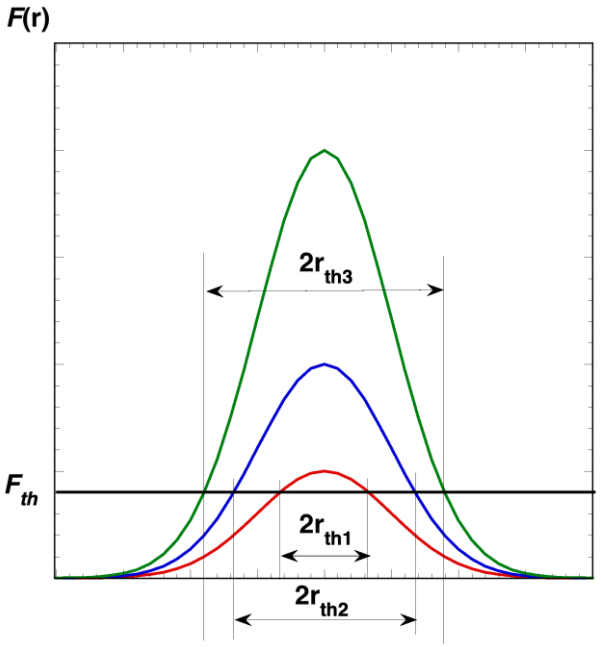

Figure 3.2: *Evolution of the footprint size as the fluence of the beam increases.*

Given a value of F_p, the size of the footprint generated on the surface of the material is given by:

$$F_{th} = F(r_{th}) = F_{max} \exp\left[-2\left(\frac{r_{th}}{r_0}\right)^2\right]$$

$$\frac{F_{th}}{F_{max}} = \exp\left[-2\left(\frac{r_{th}}{r_0}\right)^2\right] \qquad 2\left(\frac{r_{th}}{r_0}\right)^2 = ln\left(\frac{F_{max}}{F_{th}}\right) = ln\left(\frac{E_p}{E_{th}}\right)$$

$$r_{th}^2 = \frac{r_0^2}{2} ln\left(\frac{E_p}{E_{th}}\right) \qquad D_{th}^2 = 2r_0^2 ln\left(\frac{E_p}{E_{th}}\right) = 2r_0^2 lnE_p - 2r_0^2 lnE_{th}$$

In consequence, if we make different footprints increasing the pulse energy and we plot D_{th}^2 as a function of $\ln E_p$ we will obtain a linear dependence. The slope is associated with the size of the laser beam and the independent term provides the damage threshold. It is important to have in mind that similar studies can be performed for different types of damage (ablation, chemical, …), obtaining the threshold energy for each one.

C) *Determination of the beam size in the 800 ps n-IR laser*

Previous ideas have been used to determine the size of the laser beam in the lasers that have been used in this work. As an example, the determination of the 800 ps n-IR laser beam size is included. We have defined a matrix of points, separated 400 μm, in which we have applied a burst of 100 pulses at 300 kHz. The evolution of the footprints in a steel surface are presented in Figure 3.3.

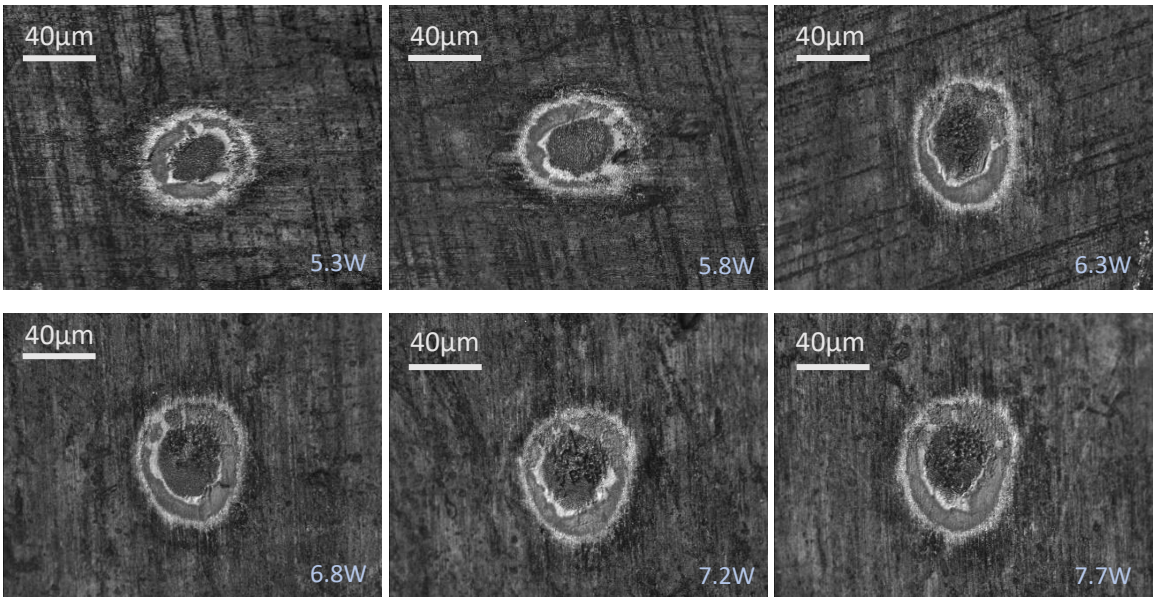

Figure 3.3: *Footprints in steel for different levels of power: 5.3W, 5.8W, 6.3W, 6.8W, 7.2W, 7.7W*

Performing the previous analysis, the dependence presented in Figure 3.4 is obtained. From the analysis of the data, we can derive that r_0=40.8 μm and D_0=81.6 μm and that in the case of the steel the damage threshold is E_{th}=13.4 μJ or F_{th}=256 mJ/cm^2.

Repeating this analysis with different materials, we have derived that for this laser D_0=80±5 μm. The shape is not completely round. Dimensions have always been taken with the biggest dimension, so we can consider that this dimension is the longest axis of the ellipsis.

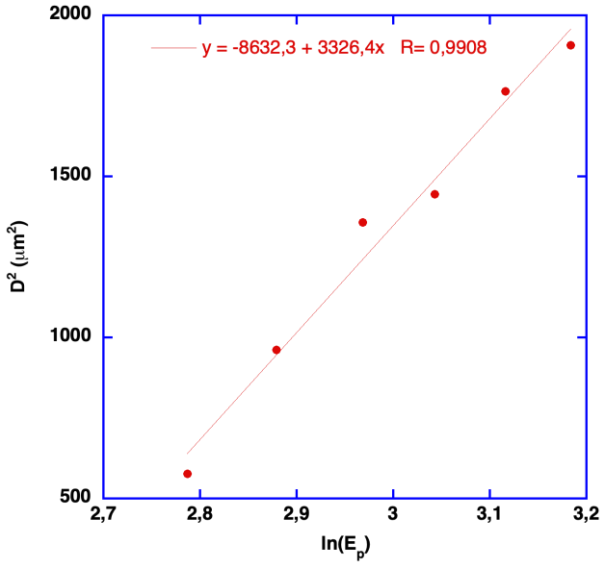

Figure 3.4: *Linear dependence of D_{th}^2 vs lnE_p used to estimate the beam size in the 800 ps n-IR laser.*

Chapter 4: Influence of laser parameters on the damage thresholds

A) Damage thresholds with the UV fs laser

It has been observed that when the UV radiation irradiates glass can generate two different kinds of defects. First, at lower energies, the laser generates an optical damage, that is reflected in a change in the color of the sample. Figure 4.1 shows an example of the aspect of a microscope slide showing this change in the color. At higher levels of energy, it has been observed that the laser starts to generate mechanical ablation on the glass surface.

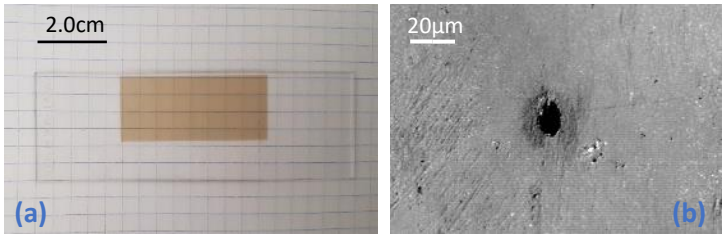

Figure 4.1: *(a) Aspect of the glass surface of a microscope slide showing the optical damage induced by the UV radiation. (b) Detail of one of the marks created by the laser when 500 pulses of 6.47 µJ are applied.*

In order to determine the damage thresholds several experiments have been performed in the burst mode applying 500 pulses in each position. The emission frequency was fixed to 200 kHz and PPD=20. In consequence, the effective frequency was 10 kHz. Figure 4.1(b) shows that the laser fingerprints have an elliptical shape. Experiments have been repeated increasing the laser energy. For each energy level, both axes of the ellipse have been measured. Figure 4.2 shows the lineal dependence of the D^2 vs ln(E_p) curves, for each axis measured in a colorless contemporary stained-glass sample. With the lineal fit of the curves the size of the laser beam is $2a$=29.5 µm and $2b$=40.4 µm and for this material $E_{th,\ mechanical}$= 5.6 µJ. A similar study performed with the fingerprints associated with the optical damage, shows that this defect is generated with lower energies, in particular, in this case $E_{th,\ optical}$= 2.5 µJ.

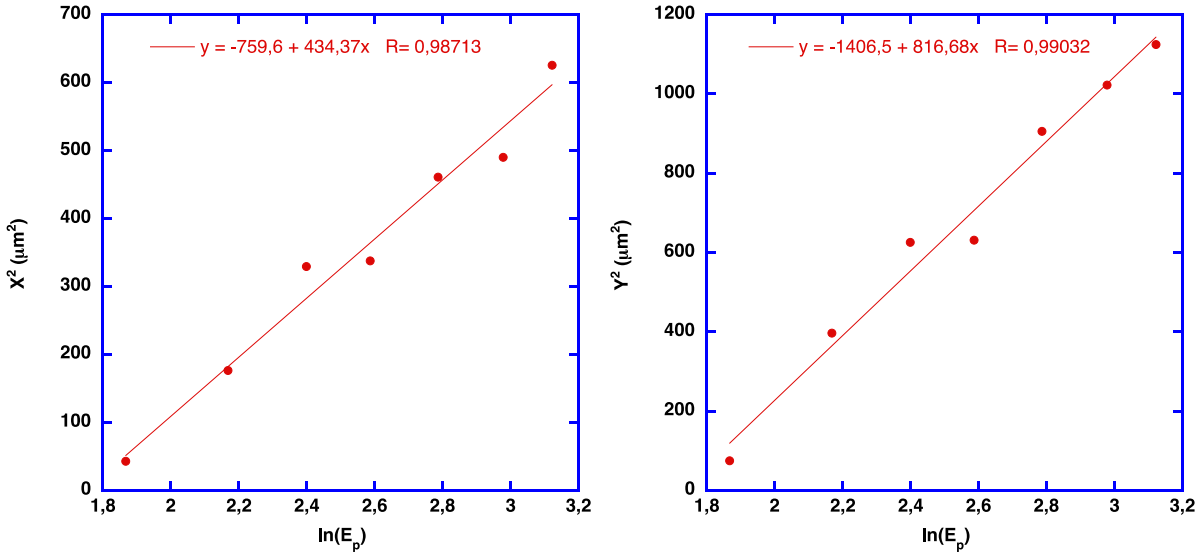

Figure 4.2: *Curves D^2 vs ln(E_p) for both axis of the mechanical marks generated by the laser treatment on a contemporary colorless stained-glass*

When the same calculations are repeated in the microscope slides, a value of $E_{th,\ mechanical}$= 6.2 μJ, slightly higher than the value obtained in the contemporary stained-glass.

B) Generation of optical damage using UV laser radiation

Several experiments have been performed on microscope slides in order to characterize the effect of the generated optical defects during the treatment with the UV radiation. As presented in Figure 4.3 two different scanning configurations have been used. In the first one, that have been called lines, the laser scans the surface in a beam scanning configuration. Laser scanning speed was selected in 150 mm/s and the effective frequency in 10 kHz in order to maintain a distance between pulses of 15 μm. Distance between scanning lines also has been fixed in 15 μm. In the second configuration, call dots, a burst mode scanning configuration has been used. In this case the laser marks a square lattice of dots with a distance between dots of 100 μm. In each position, the laser applies 500 pulses of the emission frequency. Depending on the effective frequency that is selected with the PPD, the real number of pulses that reach the samples is proportional to the selected frequency. For instance, if PPD=100, f_{ef}=2kHz and the number of pulses in each position is 5. If PPD =10, f_{ef}=20 kHz and the number of pulses in each position increases up to 50. Figure 4.4 shows an optical image of the surface of the glass after these two treatments in a glass that was processed with an energy of 2,0 μJ/pulse. In all the cases, the pulse duration was fixed to 238 fs, PPD=20, f_{ef}=20 kHz and the effective number of pulses in each position was 25.

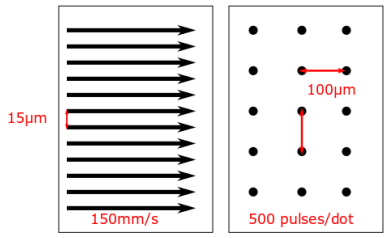

Figure 4.3: *Laser scanning configurations used to study the effects of the optical damage.*

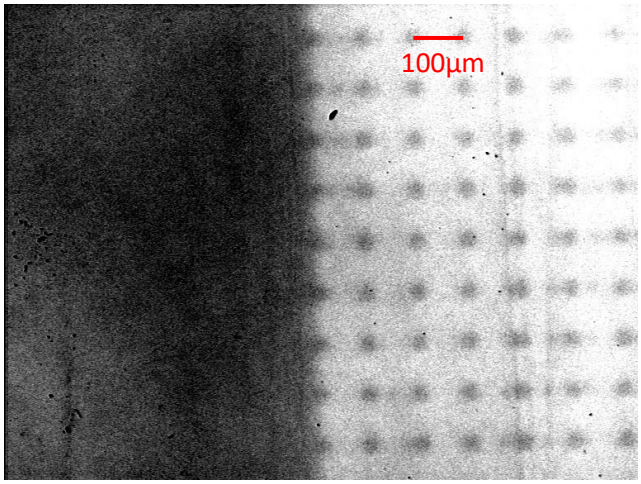

Figure 4.4: *Optical micrograph of a glass surface processed with the two configurations presented in Figure 4.3 with Ep=2.0 μJ/pulse.*

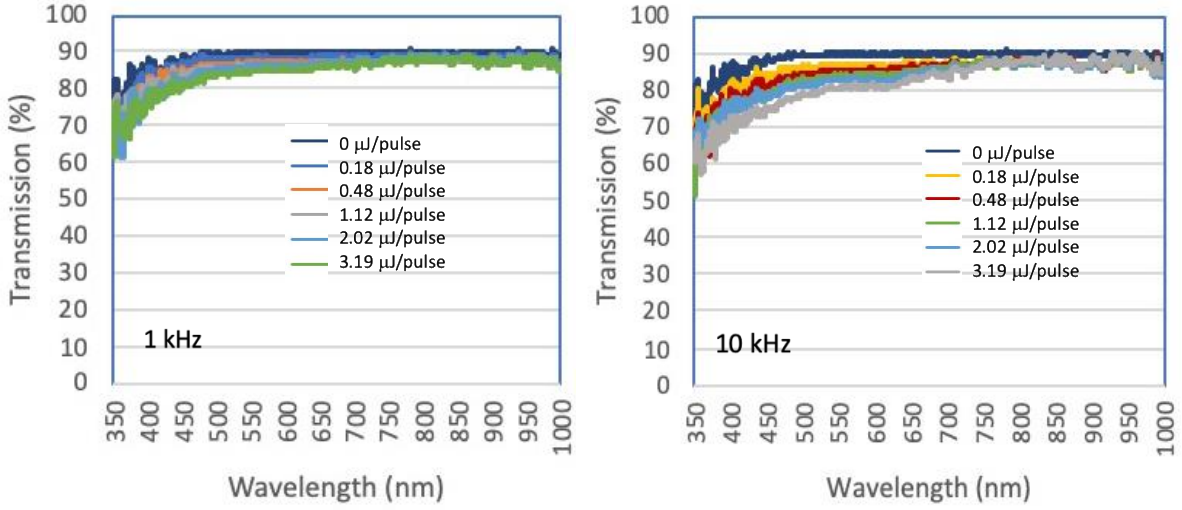

Figure 4.5: *Transmittance spectra of glasses processed in a burst configuration, with two different frequencies. Higher frequency means higher number of pulses.*

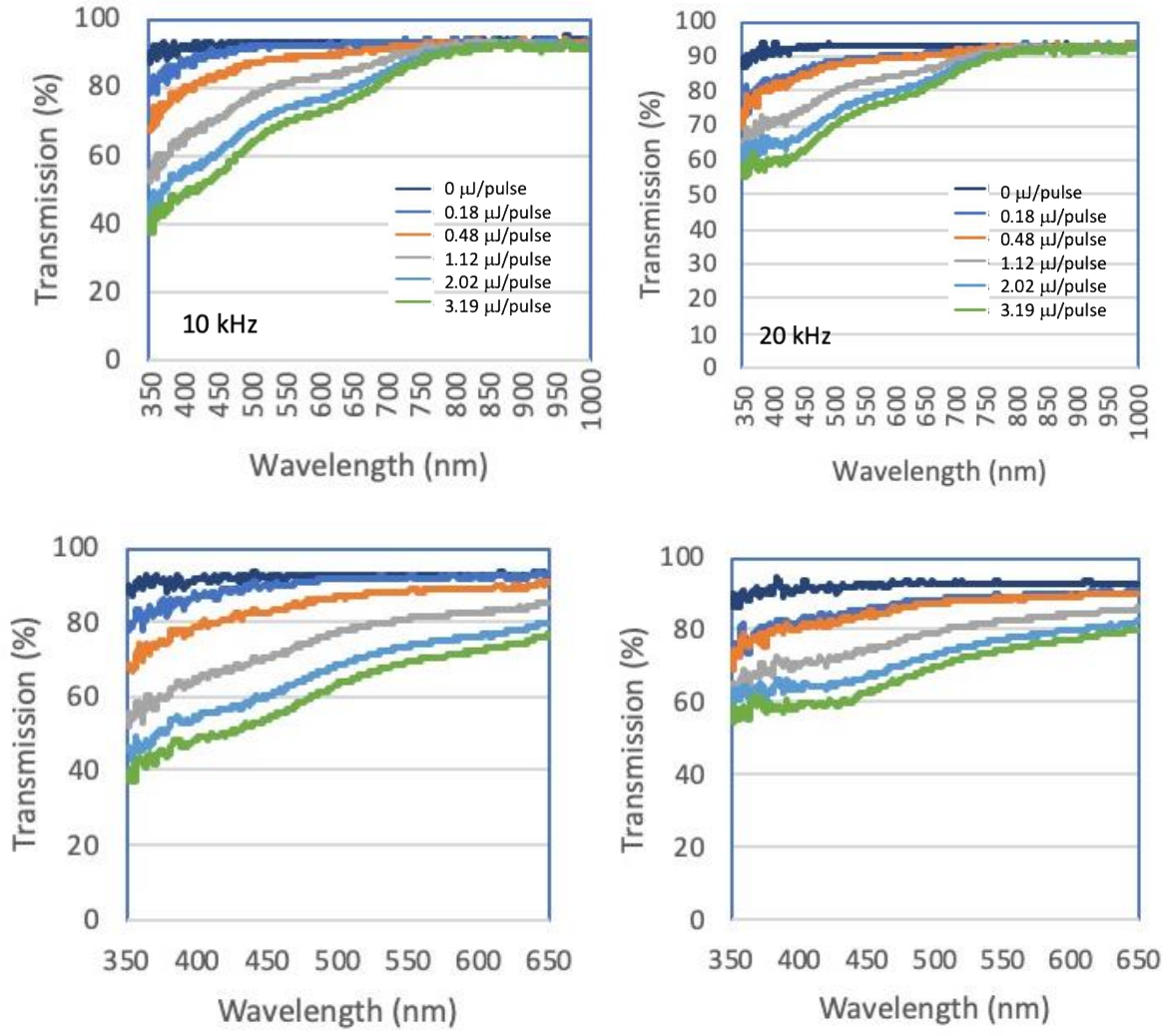

Figure 4.6: *Transmittance spectra of glasses processed with the beam scanning configuration, with two different frequencies. The second raw shows the region of the spectra between 350 and 650 nm.*

Figure 4.5 shows the transmittance spectra of several glasses processed in burst mode with increasing values of E_p. It is observed that the spectra evolve to lower transmittance values, mainly in the region with wavelengths lower than 750 nm. This reduction increases while the radiation approaches the UV region. The effect is also higher when the effective frequency increased because the number of pulses in each position was also higher.

When the surface has been scanned with the line configuration the effect of the laser treatment is higher. The transmittance spectra are presented in Figure 4.6. Transmittance values are lower for wavelengths lower than 850 nm, in the UV and visible range. Absorption in the UV range increases while the pulse energy does. This means that if a laser cleaning protocol requires repeat a given process several times, in each step, the absorption will be higher and the effect of the laser will increase. Comparing the experiments performed at the two frequencies, effects are stronger at 10 kHz than at 20 kHz. This is due to the fact that when the frequency increases, the distance between pulses in a scanning line is higher reducing the total energy deposited on the sample surface.

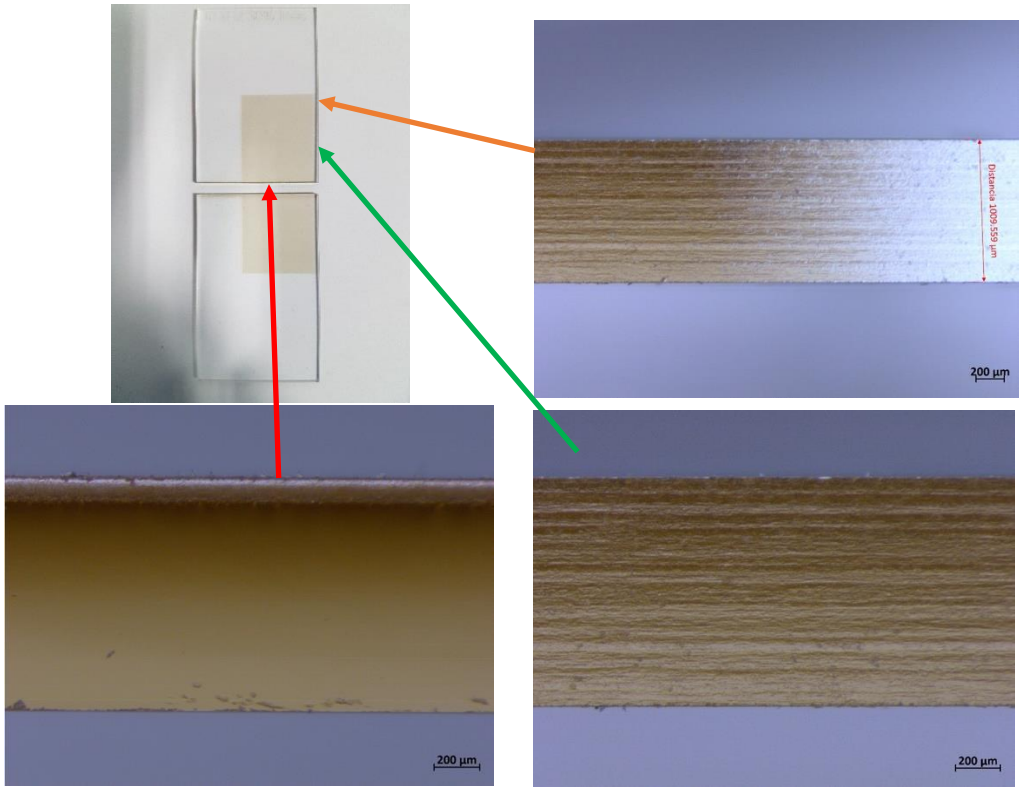

Figure 4.7: *Photograph of the sample processed with a beam scanning configuration with Ep=5.32 µJ/pulse and 10 kHz and optical micrographs of the three sections indicated in the figure.*

Some samples have been cut with laser and the cross section has been observed with optical microscopy. Photographs obtained in a sample processed with an energy of 5.32 µJ/pulse are presented in Figure 4.7. The sample was cut in two pieces using the laser. The three images have been taken in the interface between the treated and not treated region (upper image, right), inside the treated region (lower image, right) and inside the cutting region (lower image, left). It is important to

notice that with these laser conditions, the change in color is not confined close to the surface, but it has been observed in the full cross-section (1 mm). While the energy is reduced to 3.19 μJ/pulse, the damage is more confined to the sample surface as it is observed in Figure 4.8

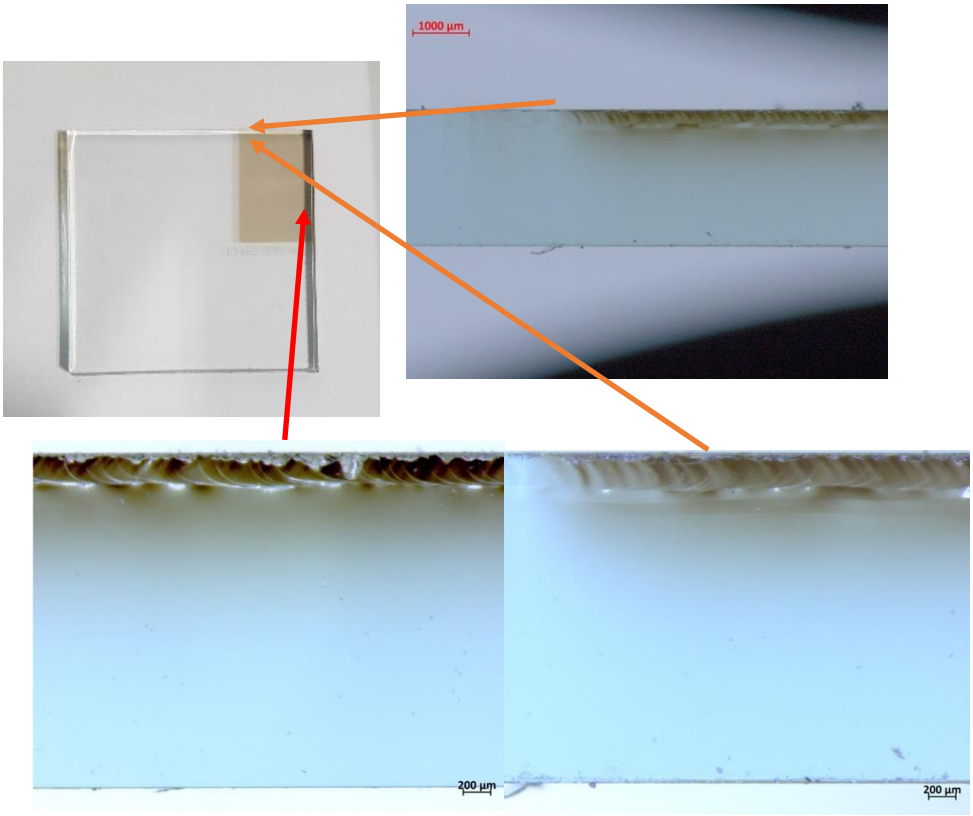

Figure 4.8: *Photograph of the sample processed with a beam scanning configuration with E_p=3.19 μJ/pulse and 10 kHz and optical micrographs of the three sections indicated in the figure.*

C) Influence of pulse duration on the damage generated by the laser

Most of the papers that study the damage threshold in different materials provide the fluence as the more characteristic parameter, but it is not evident that this magnitude should be the relevant one. As this laser allows to modify the pulse duration, we can make experiments with different pulse durations in order to analyze if the damage threshold depends or not on it. If the damage threshold does not depend on the pulse duration, fluence should be the characteristic magnitude. If it is proportional, the irradiance should be the more adequate magnitude.

The values of pulse duration that have been measured are those included in Table 4.1. The value for $E_{th,mechanical}$ clearly show a dependence on the pulse duration, a clear indication that the fluence is not the parameter that defines the damage threshold. But also, the relation between $E_{th,mechanical}$ and pulse duration is not linear, it is closer to a potential dependence with an exponent close to 1.4, as it is shown in Figure 4.9. In consequence, irradiance is not also the correct magnitude that defines the damage threshold.

Pulse duration	Multiplicative factor	$E_{th,mechanical}$ (μJ/pulse)
238 fs	1	6,2
357 fs	1.5	8,9
476 fs	2	14,8
595 fs	2.5	21,0
714 fs	3	28,9

Table 4.1: *Values of pulse duration that have been analyzed.*

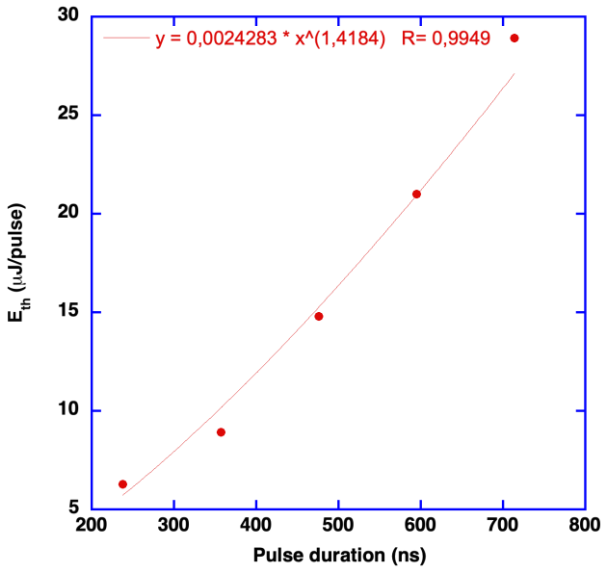

Figure 4.9*: Dependence of E_{th} on pulse duration.*

D) Influence of laser frequency on damage thresholds

Experiments have been performed at 10 kHz and at 1 kHz with the objective of determining if the change in frequency affects the measured damage thresholds, at least in this range of frequencies where heat accumulation is avoided.

Figure 4.10 shows the size of the marks created by the laser treatment when E_p=22.7 μJ, a value that is higher than the mechanical threshold, is selected for both frequencies, 1 kHz (left) and 10 kHz (right). In both cases the effect on the sample surface is very similar. Calculations provide Eth, mechanical=6.2 μJ in the case of 10 kHz and 6.4 μJ in the experiments with 1 kHz.

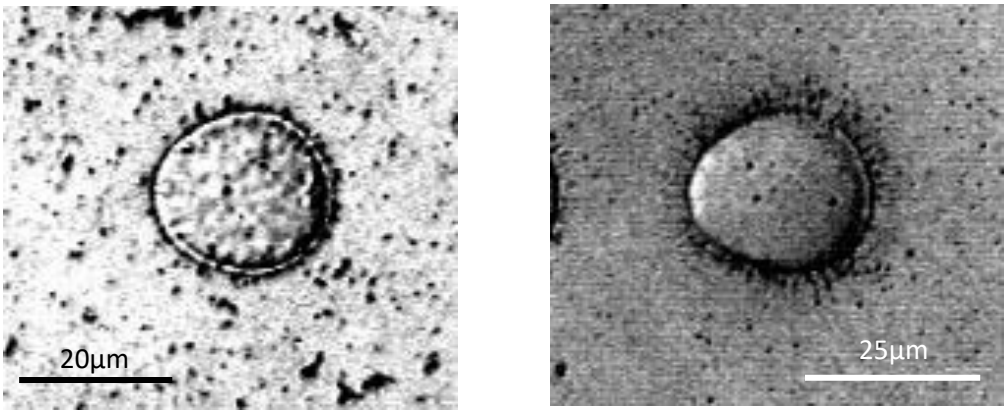

Figure 4.10: *Size of the marks created by the laser when Ep=22.7 μJ. Left 1 kHz, right 10 kHz.*

The damage threshold for the optical damage has also been calculated. In this case, a slight difference has been measured, 1.9 μJ when the effective frequency is 10 kHz and 1.4 when the frequency is reduced to 1 kHz.

Chapter 5: Influence of glass color on the damage thresholds in contemporary stained-glass

In this chapter, the damage thresholds have been measured in six contemporary stained-glass with different colors. Mechanical damage has been established in all the glasses. Optical one is more complicate to be determined because due to the low contract of the mark generated by the laser with the color of the glass it is not possible to measure the size of the affected zone.

Initially, the optical properties of the samples were determined by measuring the transmittance spectra. Results are presented in Figure 5.1 for the six samples: blue, colorless, green, purple, red and orange. One important issue is that the colorless glass is different that the sample used in Chapter 4.

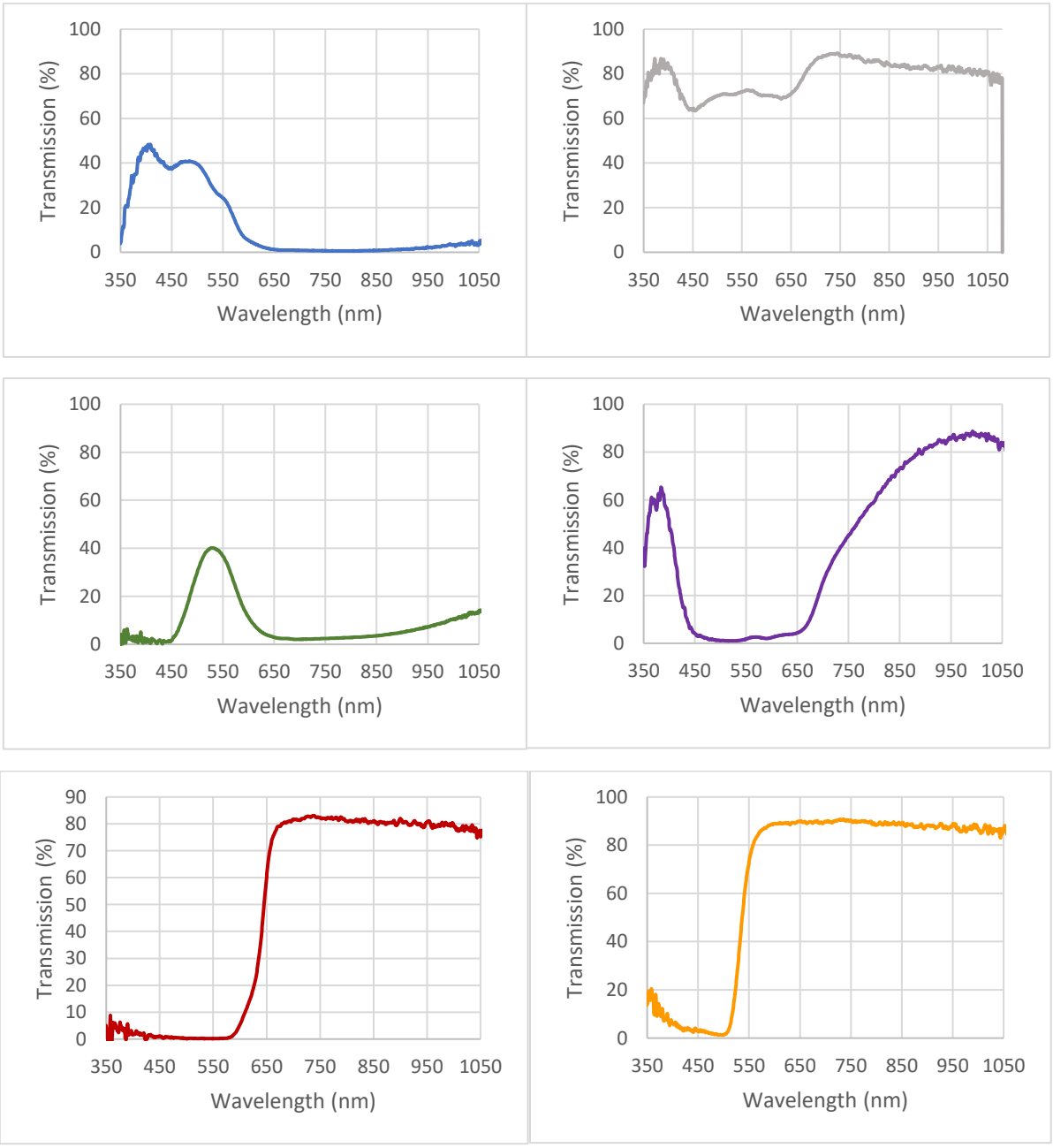

Figure 5.1: *Transmittance curves measured on the blue, colorless, green, purple, red and yellow glasses.*

It has been observed that when the UV radiation irradiates glass can generate two different kinds of defects. These transmittance spectra show that the percentage of energy transmitted in the UV range is very low in the six glasses, much lower than in the case of the IR radiation, where transmittance values higher than 80 % is observed in all the glasses. Apart from the level of energy that it is absorbed in each wavelength, it is important to have in mind that interaction with IR radiation has a high level of thermal component, while in the case of UV laser, the interaction is mainly photochemical.

A) Response to 800 ps IR radiation

In order to identify the phenomenology that it is observed when the IR radiation is used, some burst treatments have been performed on the red (high transmittance at 1064 nm) and green (low transmittance) glasses. The 800 ps n-IR laser only can operates at frequencies higher than 200 kHz. The burst mode has been selected in order to separate the temporal and the spatial pulse overlapping during the laser treatment. As it has been presented in Chapter 3, the beam size is 81.6 μm. For this reason, a burst configuration with a distance between pulses of 200 μm was selected. The maximum E_p value that is available with this laser is 24 μJ (F_p=0.49 J/cm^2).

Several experiments have been performed applying the laser directly on the glass. Areas of 2 x 2 mm^2 have been treated with a distance between spots of 200 μm. Different experiments have been performed increasing the number of pulses in each position in steps of 200. It has been observed that this energy level is below the ablation threshold in the red glass because no damage is observed even if the number of pulses increases up to 10000. The phenomenology in the green glass is different. The highest absorption is reflected in an increase in the surface temperature during the laser treatment that leads to the generation of cracks. The thermo-camera model used was Thermo Cam P25, Teledyne FLIR Systems, USA. The accuracy of the camera is 2ºC and its measuring frequency is 50 Hz. This means that an image is taken every 20ms and the given result is the average temperature of the zone during this period. Figure 5.2 shows the evolution of the surface temperature in both glasses during treatments of 200 and after having repeated the treatment five times. In the case of the red glass, the maximum temperature increase was 3.9ºC. This increases until 100.9 ºC when the same laser treatment is performed on the green glass. Also Figure 5.2.b shows the aspect of the surface of the green glass after having applied 5000 pulses in each position. It is observed that the evolution of the damage increases while the laser treatment evolves, with an evolution similar to the increase of temperature on the glass during the laser treatment.

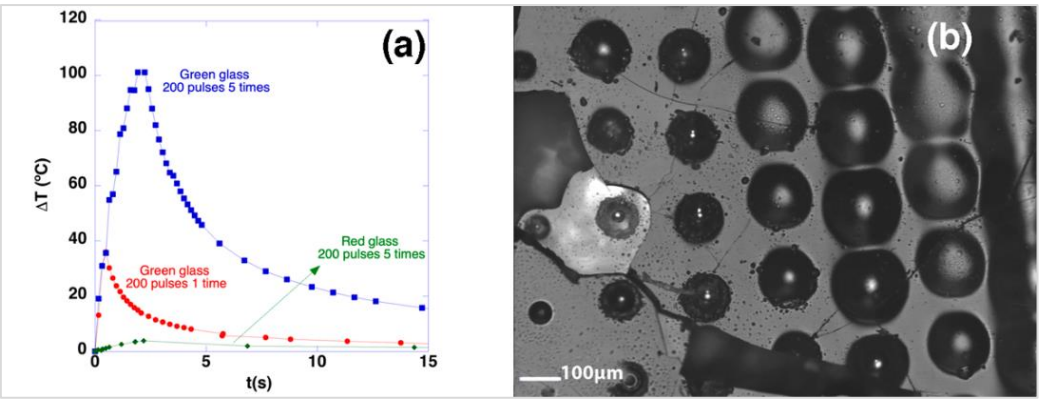

Figure 5.2: *(a) Temperature increase recorded with a thermal camera for approximately 30 s on the glass surface during several laser treatments (series of 200 pulses in each position) performed on the green and red glasses. (b) SEM micrograph of the surface of the green glass after direct laser irradiation with 5000 pulses in each position. The distance between two positions is 200 μm. The laser scans in the vertical direction of the image, starting on its left lower corner and showing that the damage level increases while the laser treatment evolves.*

This behavior also produces an increase of the thermomechanical stresses on the glass, a source of additional possibility for crack generation. These temperatures increases are higher because the frequencies available in this laser are very high producing a high level of heat accumulation. For these reasons, we have considered that a UV laser with lower available frequencies will be a more adequate selection for developing laser cleaning protocols.

B) Damage thresholds using the UV fs radiation

As it was observed in Figure 5.1, the level of energy absorption is higher in the UV range of the spectra. For this reason, before using the UV laser it is important to define which is the level of damage thresholds using this laser for the six different types of contemporary glasses. It is important to have in mind that this laser allows to work with low frequencies, what reduces the amount of heat accumulation during the laser treatment.

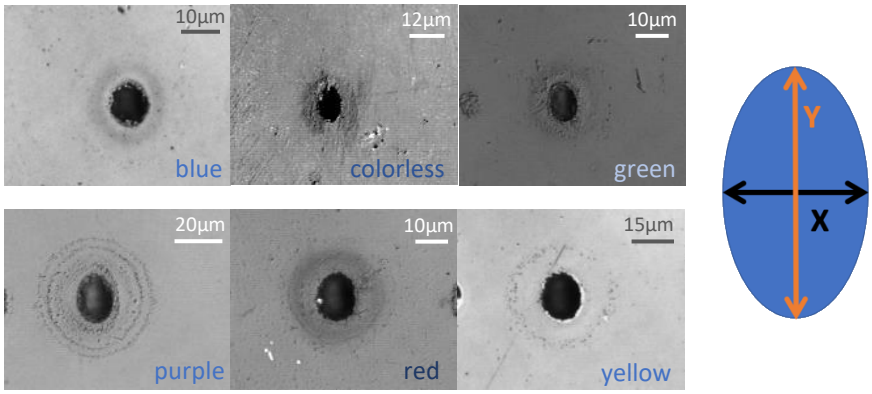

Figure 5.3: *Size of the marks generated by the laser after a burst mode, applying 25 pulses in each position with E_p=6.47 µJ and a frequency of 10 kHz in the blue, colorless, green, purple, red and yellow glasses. The diagram shows the definition of the axis that have been used in this work.*

Figure 5.3 shows the fingerprints generated by the laser in the six glasses after having applied in each position 25 pulses with E_p=6.7 µJ and a frequency of 10 kHz. Clearly, this level of energy is higher than the ablation threshold in the six materials.

In Chapter 4, it was shown that this laser can generate mechanical and optical damages on the glass surface. The optical damage threshold could be measured on the colorless glass because it was very easy to detect it due to the change in color of the sample. This cannot be detected in some of the other glasses because the color contrast is lower. For this reason, we will focus on the determination of the mechanical damage threshold.

Marks presented in Figure 5.2 confirm observations presented in Chapter 4. The laser beam is elliptical. To determine $E_{th,mechanical}$ we have been measuring the evolution of the bigger axis of the ellipsis when the laser power increases.

Table 5.1: *Values of $E_{th,mechanical}$ in the six contemporary glasses for experiments with three number of pulses: 100, 500 and 1000 pulses/position.*

Eth (µJ/pulse)	Blue	Colorless	Green	Purple	Red	Yellow
5 pulses	5.4	6.4	6.2	5.3	5.3	4.0
25 pulses	4.7	5.6	6.2	4.4	4.5	4.0
50 pulses	2.6	5.3	6.2	4.2	4.2	2.8

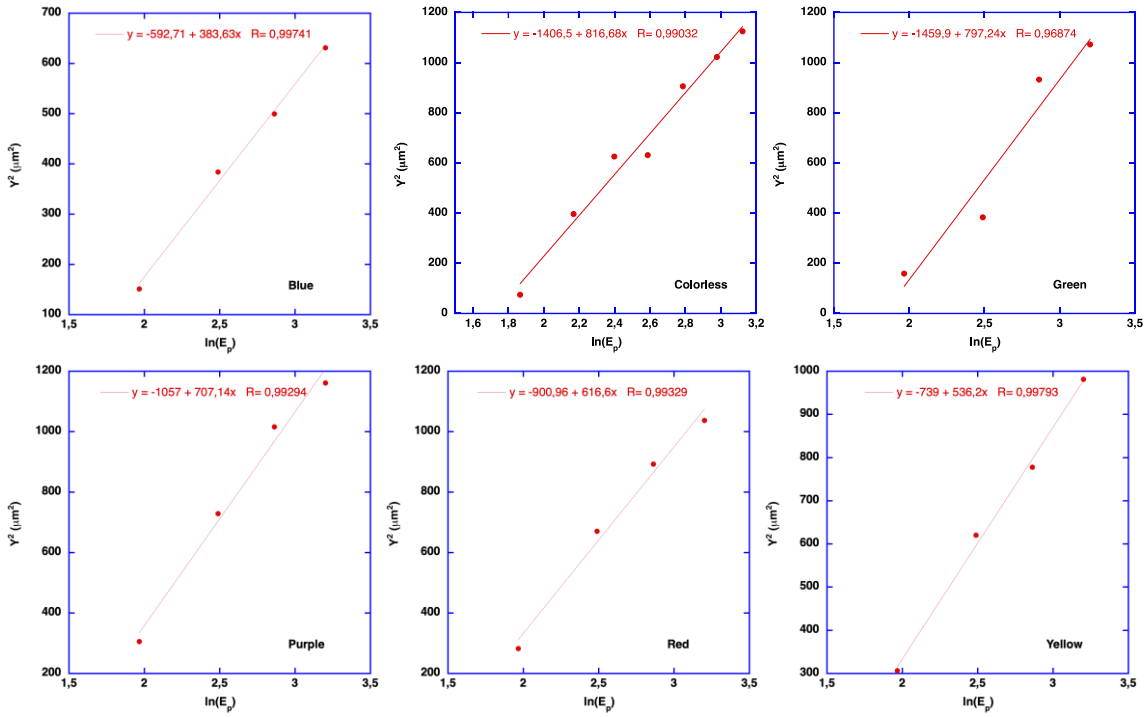

Figure 5.4: *Curves D^2 vs ln(E_p) for both axis of the mechanical marks generated by the laser treatment after having applied 25 pulses with Ep=6.7 µJ/pulse*

Figure 5.4 shows the plots D^2 vs ln(E_p) for the six glasses when a burst configuration is used with a distance between positions of 100 µm. In each position, 500 pulses at an affective frequency of 10 kHz, have been applied. The data of the mechanica thresholds are collected in Table 5.1. Also the values obtained when 5 or 50 pulses are also collected in the same table. The highest values are obtained in the green and colorless samples, while similar values are obtained in the other four glasses. In most of the cases the values of the damage thresholds decrease when the number of pulses increases.

Also it is important to notice that there is not a full correlation between the data presented in Table 5.1 and the transmitance values in the UV region that can be observed in Figure 5.1.

C) Optical damages using the UV fs laser

As it was mentioned, the determination of the damage threshold for optical damage cannot be done applying the D^2 method because the color contrast is too low in the colored glasses. Figure 5.5 shows the aspect of some glasses after laser treatment. Clearly, it is possible to detect the changes generated by the laser in the colorless samples and also some affection can be seen in the green one, but it is more complicate to see in the other samples.

Figure 5.5: *Aspect of the samples after laser treatment.*

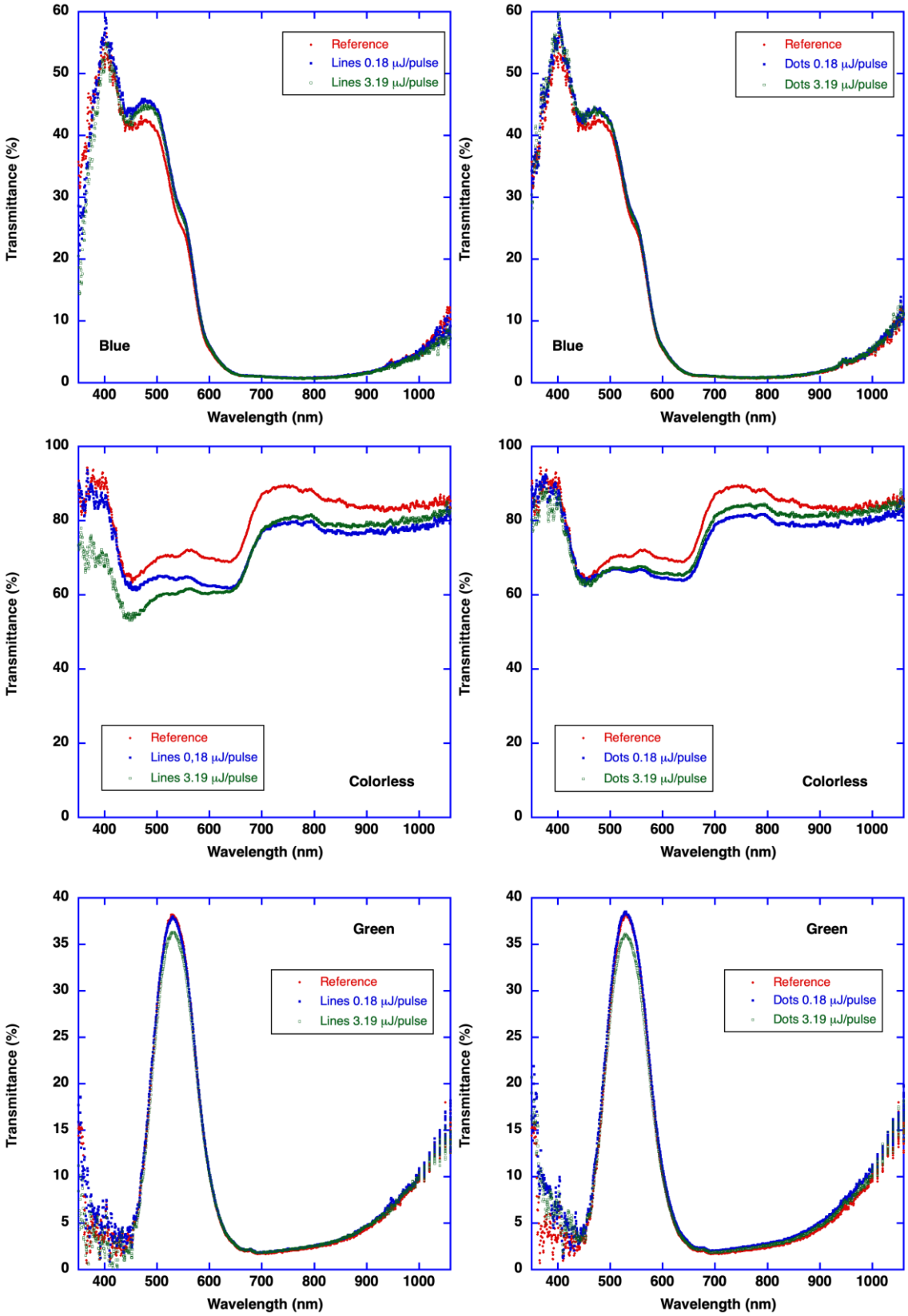

Figure 5.6: *Evolution of the transmittance spectra in the blue, colorless and green samples. Left: measurements after laser beam scanning treatments. Right: burst configuration.*

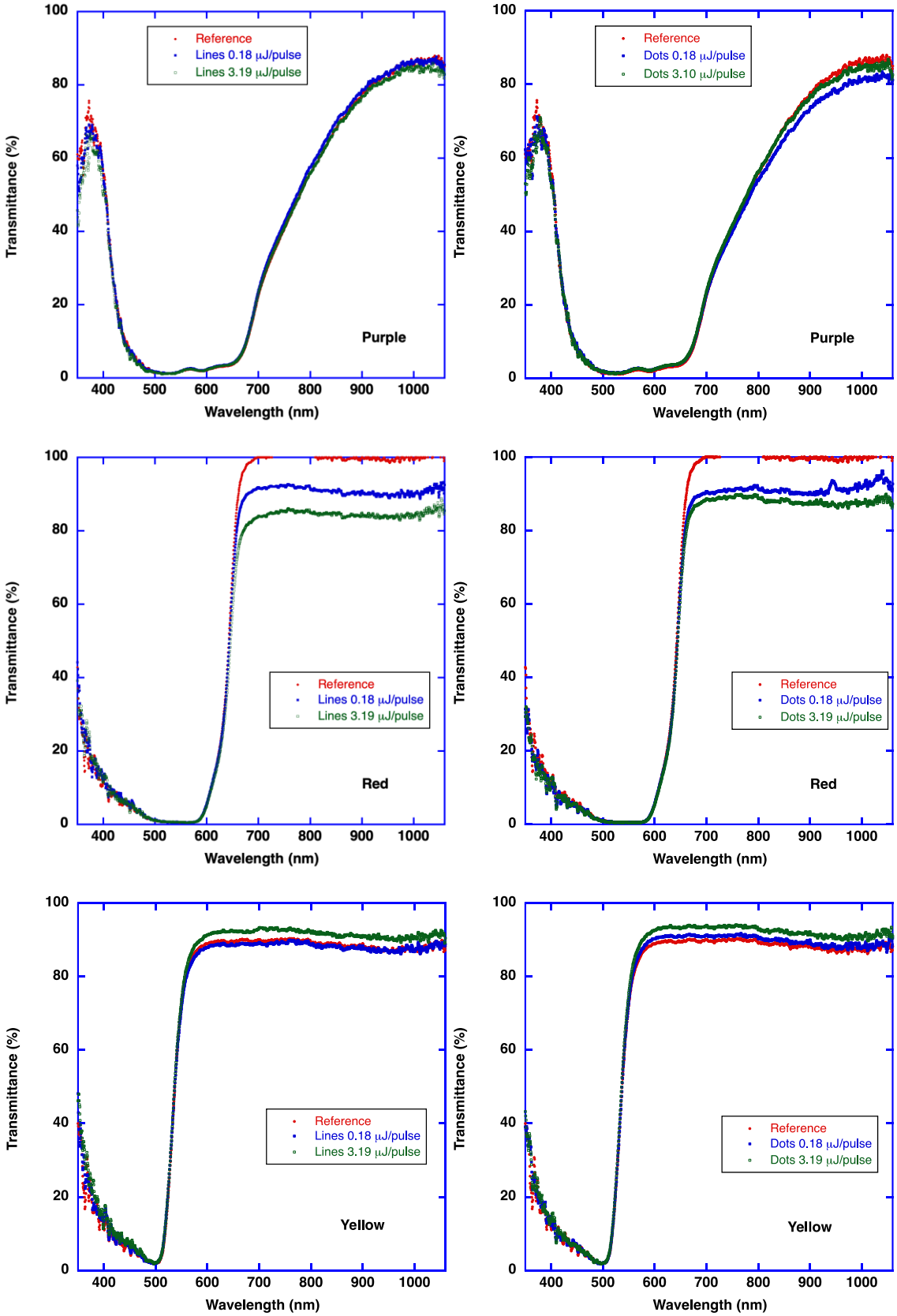

Figure 5.7: *Evolution of the transmittance spectra in the purple, red and yellow samples. Left: measurements after laser beam scanning treatments. Right: burst configuration.*

In consequence, it is not possible to determine which is the energy threshold for optical damage using the standard procedures in colored glasses, but it is also important to look for some alternative that allows determining if the UV radiation can produce any optical damage or not.

We have explored the posibility of comparing the transmitance spectra before and after laser treatment. Results are presented in Figure 5.6 and 5.7 for the six glasses, where the same treatments that were used in Chapter 4 have been applied in this case. A treatment in which the burst mode is used applying 25 pulses in each position (Distance between positions 100 μm) with two levels of energy per pulse (0.18 μJ/pulse and 3.19 μJ/pulse). A second treatment where a beam scanning configuration is applied also with the same two levels og energy per pulse and using a laser scanning speed of 150 mm/s, an effective frequency of 10 kHz and a distance between scanning lines of 15 μm.

In the case of the blue glass, a slight increase of the transmittance values is observed in the shoulder that appers in the range between 440 and 560 nm. This increase does not depend on the the level of the energy per pulse, at least in the range of analysed energies, indicating that the damage threshold is lower than 0.18 μJ/pulse in this sample. Changes induced by the UV laser are higher in the beam scanning configuration.

Changes are more evident in the colorless samples, as it can be also observed in Figure 5.8. Initially, a reduction of the transmittance values at wavelengths higher than 440 nm is observed. This is the case of the two treatments with the burst configuration and with the lower level on energy in the beam scanning configuration. When 3.19 mJ/pulse is reached, then the transmittance in the UV region starts to decrease in a similar way to the microscope slides behaviour presented in Chapter 4.

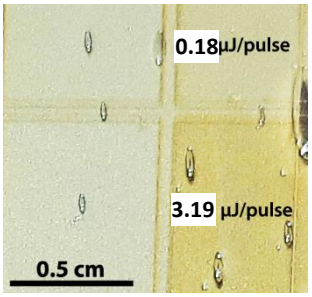

Figure 5.8: *Aspect of the colorless samples after the four treatments (right: beam mode configuration, left: burst mode)*

In the case of the green glass, the main effect is a reduction on the transmittance values in the peak at 530 nm. This reduction is observed in both configurations but only at the highest energy level, indicating that the damage threshold is between 0.18 μJ/pulse and 3.19 μJ/pulse.

The purple glass do not show an evident effect. Only a slight modification is observed at wavelengths higher than 800 nm in the beam scanning configuration, but there is not and evident trend because the effect is higher with lower enegy values. This differences can be associated to the fact that small variations are observed in the high transmittance regions of the spectra due to presence of bubbles inside the glass.

In the case of the red glass, the main differences are associated with a reduction on the transmittance values at wavelength values higher than 650 nm. The reduction increases while the energy per pulse increases. By contrast, in the yellow glass, this high trasmittance region starts in 550 nm and the effect of the laser only can be detected at higher energy values. In this case the effect is the opposite, with

0.18 μJ/pulse there is not effect, while the energy increases up to 3.19 μJ/pulse the transmittance increases.

All these observations can be collected in Table 5.2, where the main observations are included.

Glass	Damage threshold	Main facts
Blue	<0.18 μJ/pulse	440nm<λ<560 nm. Independent of the energy level, increase of transmittance
Colorless	<0.18 μJ/pulse	In the full range, reduction of transmittance
Green	Between 0.18 and 3.19 μJ/pulse	Only at the peak, reduction of transmittance
Purple	>3.19 μJ/pulse	No effect
Red	<0.18 μJ/pulse	In the high transmittance region, reduction of transmittance
Yellow	Between 0.18 and 3.19 μJ/pulse	In the high transmittance region, increase of transmittance

Table 5.2: *Main conclusions from transmittance data*

Chapter 6: Definition of laser cleaning protocols

The results obtained in the previous chapter have been used to define a cleaning protocol that avoids damaging the samples. This has been performed on microscope slides samples that have been painted with permanent ink using a Staedtler Lumocolor permanent marker. Analysis with confocal microscopy show that the thickness of the ink ranges from 10 to 20 μm. Figure 6.1 shows the aspect of a sample after having applied the ink and after having tested several laser cleaning protocols.

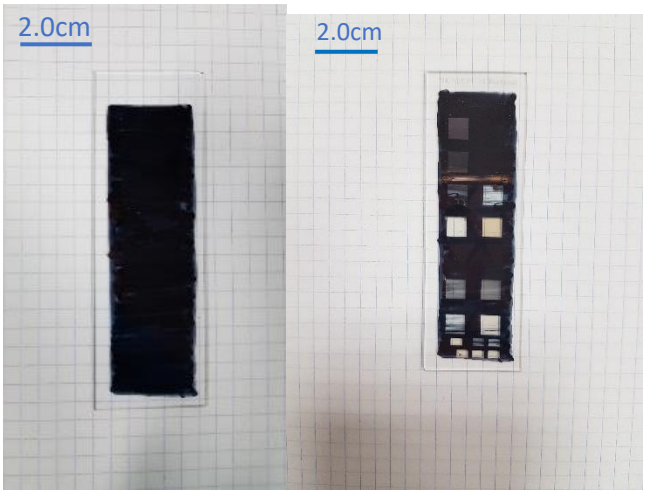

Figure 6.1: *Photograph of the sample after having being painted with permanent ink and after having performed some laser cleaning processes.*

As it was indicated in Chapter 2, in order to make the laser cleaning treatments it is important to have in mind that if glass is placed on top or a surface and laser can reach this surface it can ablate nanoparticles from the surface of the material that can be penetrate inside the glass surface. This phenomenon, called Laser reverse transfer is used frequently to deposit metallic layers on top of the glass surface. For this reason, samples have been placed inside an aluminum sample holder (Figure 6.2) that allows to maintain the bottom surface of the glass with a gap of approximately 2 mm above the surface where the glass is placed.

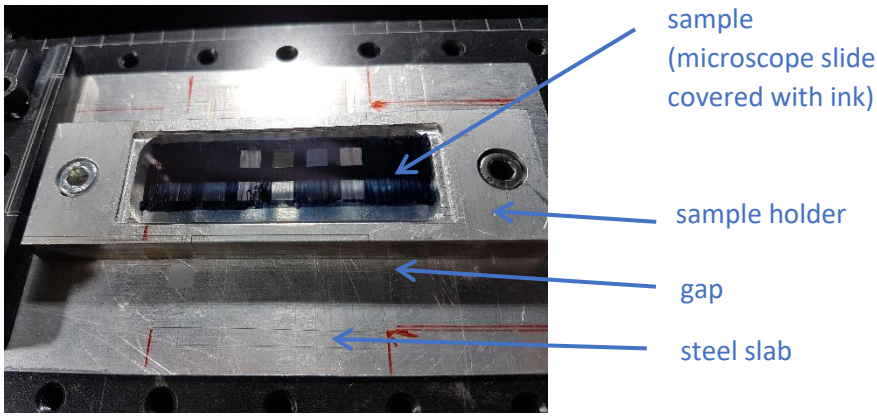

Figure 6.2: *Arrangement designed to make the laser experiments to maintain a gap bellow the bottom glass surface.*

Initial treatments have been performed in areas of 5 mm x 5 mm following the same scanning configurations that have been presented in previous chapters, burst mode (dots in Figure 6.3) and beam scanning (lines in Figure 6.3).

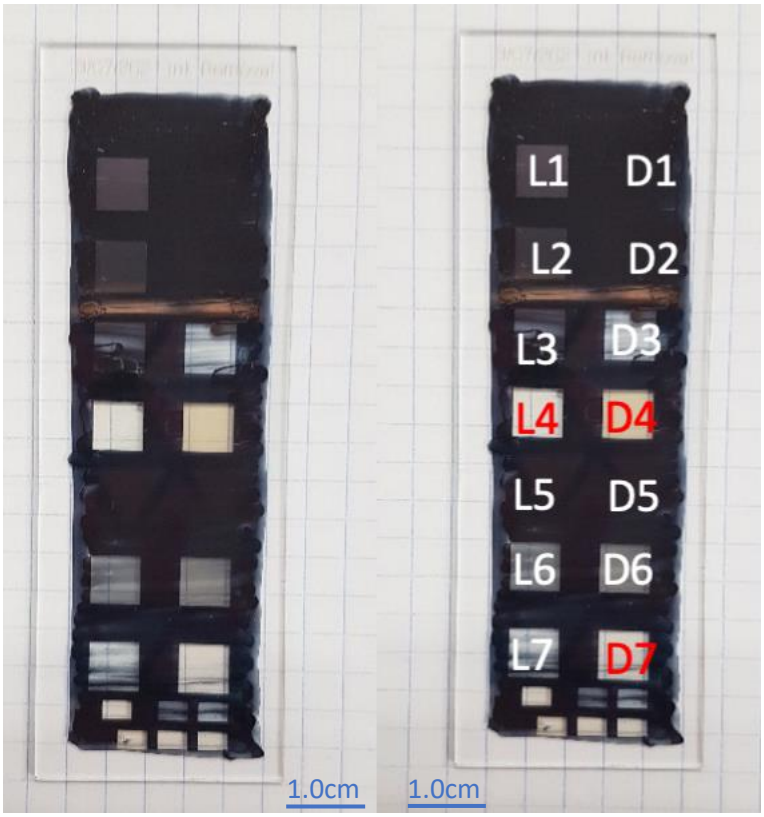

Figure 6.3: *Aspect of the sample after laser cleaning treatments (left) and names that have been assigned to each treatment (right)*

Table 6.1 shows the laser parameters used in the cleaning protocols developed using the burst mode configuration. In all the case, the pulse duration was 238 fs and the frequency was 10 kHz or lower to avoid heat accumulation [Maingi 2022] and the pulse energy was lower than the damage thresholds determined in previous chapters. D1 and D2 have been performed with two levels of energy but with a distance between positions of 100 μm, higher than the beam size. Level of amount of ink that is removed is very low.

Treatment	Pulse duration (ps)	Frequency (kHz)	Number pulses in each position	Distance between positions (μm)	E_p (μJ)	Number of times
D1	238	1	3	100	0.18	10
D2	238	10	25	100	0.18	10
D3	238	10	25	15	0.48	1
D4	238	10	25	15	0.48	5
D5	238	10	25	15	0.18	1
D6	238	10	25	15	0.18	100
D7	238	10	25	15	0.48 0.28 0.23 0.18	1 1 1 2

Table 6.1: *Laser parameters used in the cleaning protocols using the burst configuration*

It increases considerably when the distance between pulses is reduced to 15 μm, lower than the beam radius. In case of D3, the process was repeated only once, but the amount of ink that is removed is high. When the process is repeated 5 times (treatment D4) ink is completely removed from the glass surface. But the glass starts to be affected by the laser treatment, probably due to heat accumulation. It was observed that change in color could be appreciated after the second time the process is repeated. Ink is completely removed after the fourth step. D5 and D6 corresponds to a new series of very light treatments (E_p=0.18 μJ) that are repeated many times, 1 and 100. A final treatment (D7) was designed starting with an initial step of with an energy per pulse of 0.48 μJ when the glass is completely covered with ink and reducing it slowly in the following steps, when the laser starts to reach directly the glass surface. With these conditions, ink is completely removed without affecting the glass.

The treatments performed with the beam scanning configuration are detailed in Table 6.2. In all the cases, the pulse duration is 238 fs and the distance between lines is 15 μm. Frequency and laser scanning speed have been adjusted to obtain a distance between pulses also of 15 μm. The two initial treatments, performed with an energy per pulse of 0.18 μJ, L1 and L2, are not enough to remove the ink, even if the process is repeated 10 times. The treatment is more effective if E_p is increased up to 0.48 μJ. With this level of energy, the ink is completely removed after 5 times and a slight alteration of the glass is observed after the fourth time the process is repeated. L5 and L6 have been performed again reducing the energy of each pulse, but in this case the process is not so effective even if the process is repeated 100 times. A final treatment (L7) was designed starting with an initial step of with an energy per pulse of 0.48 μJ when the glass is completely covered with ink and reducing it slowly in the following steps, when the laser starts to reach directly the glass surface. Only 5 steps are not enough to completely remove the ink but the glass is not affected so, it seems that it is possible to increase the number of steps.

Treatment	Pulse duration (ps)	Frequency (kHz)	Laser scanning speed (mm/s)	Distance between lines (μm)	E_p (μJ)	Number of times
L1	238	1	15	15	0.18	10
L2	238	10	150	15	0.18	10
L3	238	10	150	15	0.48	1
L4	238	10	150	15	0.48	5
L5	238	10	150	15	0.18	1
L6	238	10	150	15	0.18	100
L7	238	10	150	15	0.48 0.28 0.23 0.18	1 1 1 2

Table 6.2: *Laser parameters used in the cleaning protocols using the laser beam scanning configuration*

A new set of experiments have been performed on rectangles of 2 mm x 3 mm. In these new set of samples, the different times the scan is repeated have been performed modifying the scanning direction. In principle a horizontal (→) and a vertical (↓) configuration have been used in different treatments. Laser parameters are presented in Table 6.3 and the aspect of the sample is presented in Figure 6.4. In treatments L8, L12 and L13, with the higher energies per pulse, the laser affects the glass surface.

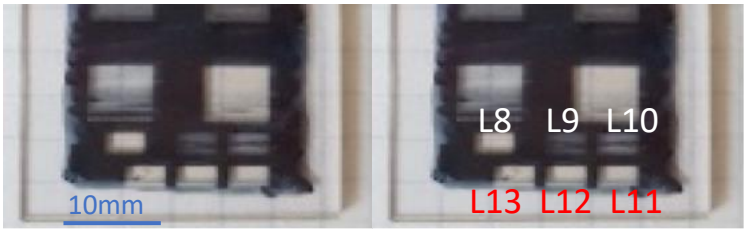

Figure 6.4: *Results of the initial experiments in rectangles of 2 mm x 3 mm*

Treatment	Pulse duration (ps)	Frequency (kHz)	Laser scanning speed (mm/s)	Distance between lines (μm)	E_p (μJ)	Number of times
L8	238	10	150	15	3.19	1 (→)
L9	238	10	150	15	0.28	3 (→→↓)
L10	238	10	150	15	0.48	1 (→)
L11	238	10	150	15	2.02	1 (→)
L12	238	10	150	15	2.72	1 (→)
L13	238	10	150	15	3.75	1 (→)

Table 6.3: *Laser parameters used in the first set of rectangles of 2 mm x 3 mm*

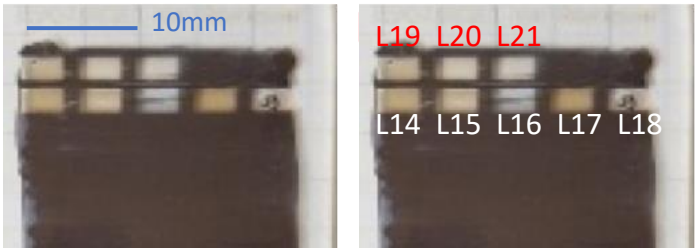

Figure 6.5: *Results of the second set of experiments in rectangles of 2 mm x 3 mm*

A new set of experiments have been performing reducing the distance between pulse in a line and the distance between lines to 10 mm (treatments L14 to L17 in Table 6.4 and Figure 6.5). In the four cases, laser is affected by the laser treatment probably due to high energy accumulation due to the reduction in the distance between pulses.

Final treatments have been performed again with distances between pulses and lines of 15 μm. In this case, the treatments have been designed performing an initial treatment with relatively high energy levels when the laser reaches the ink and the following treatments, when the laser can reach the glass surface with very low energy values. Figure 6.6 shows the aspect of the surface after having performed

the treatment L21 with an initial step using E_p=2.02 μJ and three additional steps with E_p=0.18 μJ. It is clear that the laser cleaning was effective without inducing any defect on the glass surface.

Treatment	Pulse duration (ps)	Frequency (kHz)	Laser scanning speed (mm/s)	Distance between lines (μm)	E_p (μJ)	Number of times
L14	238	10	100	10	3.19	1 (→)
L15	238	10	100	10	2.02	1 (→)
L16	238	10	100	10	0.48	1 (→)
L17	238	10	100	10	1.12	2 (→→)
L18	238	10	150	15	3.19	1 (→)
L19	238	10	150	15	3.19 0.28	1 (→) 9 (#)
L20	238	10	150	15	3.19 0.18	1 (→) 1 (↓)
L21	238	10	150	15	2.02 0.18 0.18	1 (→) 1 (→) 2 (#)

Table 6.4: *Laser parameters used in the second set of rectangles of 2 mm x 3 mm. # indicates that the orientation changes 90º each step.*

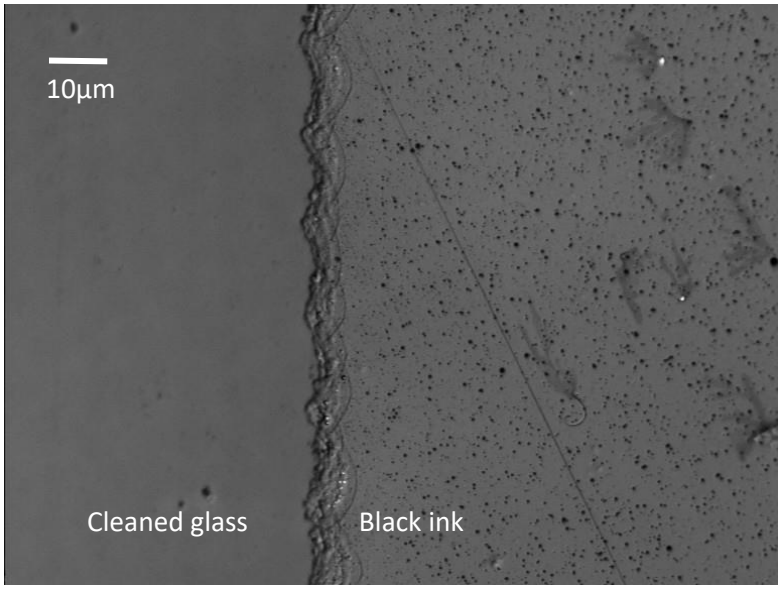

Figure 6.6: *Image obtained with the confocal microscope (objective x50) after having applied condition L19 (Left: cleaned glass, right: black ink)*

Chapter 7: Conclusions

The main conclusions of this work are the following:

- It has been established that UV radiation with a pulse duration of 238 fs can induce mechanical and optical damage on the glass samples. In colorless glasses, it is possible to apply Liu method to measure the laser beam size and the damage energy threshold.
- Depending on the glass composition, $E_{th,\ mechanical}$ values of the order of 5.5-6 μJ have been measured, while $E_{th,\ optical}$ is lower, in the range of 2.5 μJ.
- In samples with different colors, Liu method is not adequate because there is not enough contrast to determine the mark generated by the laser. In this case, information about the level of damage threshold has been determined analyzing the evolution of the transmittance spectra. Differences between six different colors have been stablished.
- Apart from these mechanical and optical damages, heat accumulation can also induce some deterioration on the glass due to thermomechanical stresses induced during the laser treatment. This is more relevant when high frequencies are used. For this reason, low frequencies values, of the order of 10 kHz are desirable to develop these laser cleaning protocols.
- It has been determined that the level of energy that induces damage on the glass depends on the pulse duration. This is an indication that irradiance is more relevant than fluence in these phenomena.
- In the range of frequencies between 1 and 10 kHz, damage thresholds do not depend on the frequency.
- Some laser cleaning protocols have been defined to eliminate a layer of permanent ink over the surface of a microscope slide. Best results have been obtained using a protocol with several steps. In the first one the objective is to eliminate as much ink as possible, without reaching the glass. In the following steps, the level of energy is lower than the optical damage threshold and the treatment can be repeated several times, changing the scanning direction in each step.

REFERENCES

Agua-Martínez, F., Solano-Rodríguez, E., Villegas-Broncano, M.A., (2022), Deterioration and degradation of Stained-glass Windows Materials, *Greatests Medieval Stained-glass Windows in Burgos*, Burgos, 2022, pp.123-128.

Ben-Yakar, A., Byer, R. L. (2004). Femtosecond laser ablation properties of borosilicate glass. *Journal of Applied Physics, 96*(9), 5316-5323.

Bonse, J. (2010). *DFG - Glass project meeting.* BAM Federal Institute for Materials Research and Testing, Working group "Pulse Laser Technologies, Laser Safety".

Carmona Tejero, N., Villegas Broncano, M.A., Fernández Navarro, J.M. (2001): "Vidrieras históricas: restauración y conservación". AR&PA 2000. Actas del Congreso Internacional "R*estaurar la memoria*", Diputación Provincial de Valladolid, Junta de Castilla y León, Valladolid, pp. 359-370.

Carmona, N., Villegas, M.A., Fernández Navarro, J.M. (2003): "Estudio comparativo del comportamiento de los sistemas de protección superficial para vidrios históricos". AR&PA 2003. Actas del Congreso Internacional de Restauración "Restaurar la memoria". *Los criterios científicos de la restauración de los Bienes Culturales: tradición y nuevas tecnologías*, Diputación Provincial de Valladolid, Junta de Castilla y León, Valladolid, pp. 337-347.

Carmona, N., Villegas, M.A., Fernández Navarro, J.M. (2004): "Protective silica thin coatings for historical glasses". *Thin Solid Films*, 458 (1-2): 121-128.

Carmona, N., García Heras, M., Gil, C., Villegas, M.A. (2005a): "Vidrios y grisallas del siglo XV de la Cartuja de Miraflores (Burgos): caracterización y estado de conservación". *Boletín de la Sociedad Española de Cerámica y Vidrio*, 44 (4): 251-258.

Carmona, N., Láiz, L., González, J.M., García Heras, M., Villegas, M.A., Saiz Jiménez, C. (2006a): "Biodeterioration of historic stained-glasses from the Cartuja de Miraflores (Spain)". I*nternational Biodeterioration and Biodegradation*, 58 (3-4): 155-161.

Carmona, N., Villegas, M.A., Fernández Navarro, J.M. (2006e): "Study of glasses with grisailles from historic stained-glass windows of the Cathedral of León (Spain)". *Applied Surface Science*, 252 (16): 5936-5945.

Carmona, N., Villegas, M.A., Fernández Navarro, J.M., (2006f): "Sol-gel coatings in the ZrO2-SiO2 system for protection of historical works of glass". *Thin Solid Film*s, 515 (4): 1320-1326.

Carmona, N., García Heras, M. , Robles, A., Villegas, M.A. (2009): "Scientific assessment of the natural weathering submitted by stained-glasses from the Cathedral of León (Spain)". En Annales of the 17th Congress of the International Association for the History of Glass, University Press Antwerp, Amberes, pp. 467-472.

Carson Pastan, E., Kurmann-Schwarz, B. (2019). Investigations in Medieval Stained-glass - Materials, Methods, and Expressions. Brill.

García Heras, M., Gil, C., Carmona, N., Villegas M.A. (2003a): "Weathering effects on materials from historical stained-glass windows". *Materiales de Construcción*, 53 (270): 21-34.

García-Heras, M., M.A. Villegas, E. Cano, F. Cortés y J.M. Bastidas (2003b): "Conservation and analytical study of metallic elements from medieval Spanish stained-glass windows". *Archeometallurgy in Europe, Asociación Italiana de Metalurgia*, Milán, pp. 381-390.

García-Heras, M., M.A. Villegas, E. Cano, F. Cortés Pizano y J.M. Bastidas (2004): "A conservation assessment on metallic elements from Spanish Medieval stained-glass windows". *Journal of Cultural Heritage*, 5 (3): 311-317.

García Heras, M., N. Carmona y M.A. Villegas (2006b): "Metallic components from historical stained-glass windows: a conservation challenge". *Ochrona Przed Korozja (Corrosion Protection*), 11: 350-353.

García-Heras, M., Montero, I. , Caen, J.M.A., Villegas, M.A. (2009): "Estudio analítico de perfiles del emplomado de vidrieras históricas de distinta cronología y procedencia". *Actas del Congreso Metal España '08*, Universidad Autónoma de Madrid y CSIC, Madrid, pp. 34-40.

Haibin, Z., Eaton, S. M., J. L., P. R. (2007). Heat accumulation during high repetition rate. *Journal of Physics: Conference Series,* 59, 682–686.

Liu, J. M. (1982). Simple technique for measurements of pulsed Gaussian-beam spot sizes. *Optics Letters,* 7(5), 196-198.

Maingi, E.M., Alonso, M.P., Angurel, L.A., Rahman, Md A., Chapoulie, R., Dubernet, S., de la Fuente, G.F. (2022) Historical staine-glass window laser preservation: The heat accumulation challenge, *Boletín de la Sociedad Española de Cerámica y* Vidrio, https://doi.org/10.1016/j.bsecv.2021.12.003

Molina, R., Ertugrul, M., Larrea, A., Navarro, R., Rico, V., Yubero, F., González-Elipe, A.R., de la Fuente, G.F., Angurel, L.A. (2021). Laser-induced scanning transfer deposition of silver electrodes on glass surfaces: A green and scalable technology. *Applied Surface Science* 556, 149673

Müller, W., Torge M., Adam, K. (1994): "Ratio of $CaO/K_2O > 2$ as evidence of a special Renish type of Medieval stained-glass". G*lastechnische Berichte Glass Science and Technology*, 67: 45-48.

Navarro, J. M. (1996). Alteration processes of medieval stained-glass windows. Study and protection treatments. *Materiales de Construcción*, 46, 242-243.

Peña-Poza, J., Conde, J.F., Agua, F., García Heras, M., Villegas, M.A. (2013): "Application of sol-gel based sensors to environmental monitoring of Mauméjean stained-glass windows housed in two different buildings at downtown Madrid". *Boletín de la Sociedad Española de Cerámica y Vidrio*, 52 (6): 268-276.

Sonia Murcia-Mascarós, P. F. (2008). A new cleaning method for historic stained-glass windows. *Journal of Cultural Heritage*, 9, 73-80.

Weber, R., Graf, T., Berger, P., Onuseit, V., Wiedenmann, M. (2014). Heat accumulation during pulsed laser. *Optical Society of America*, 22(9).

Villegas, M.A., Agua, F., Conde, J. F., García Heras, M. (2008): "Historical glasses: approaches, degradation and preservation". *Archaeologia Polona*, 46: 295-316.